



HAL
open science

Nash strategies for the inverse inclusion Cauchy-Stokes problem

Abderrahmane Habbal, Moez Kallel, Marwa Ouni

► **To cite this version:**

Abderrahmane Habbal, Moez Kallel, Marwa Ouni. Nash strategies for the inverse inclusion Cauchy-Stokes problem. *Inverse Problems and Imaging*, 2019, 13 (4), pp.36. 10.3934/ipi.2019038. hal-01945094

HAL Id: hal-01945094

<https://inria.hal.science/hal-01945094>

Submitted on 5 Dec 2018

HAL is a multi-disciplinary open access archive for the deposit and dissemination of scientific research documents, whether they are published or not. The documents may come from teaching and research institutions in France or abroad, or from public or private research centers.

L'archive ouverte pluridisciplinaire **HAL**, est destinée au dépôt et à la diffusion de documents scientifiques de niveau recherche, publiés ou non, émanant des établissements d'enseignement et de recherche français ou étrangers, des laboratoires publics ou privés.

Nash strategies for the inverse inclusion Cauchy-Stokes problem

Abderrahmane HABBAL¹, Moez KALLEL² and Marwa OUNI²

¹ Université Côte d'Azur, Inria, CNRS, LJAD, UMR 7351, Parc Valrose, Nice 06108, France.

²Laboratoire LAMSIN, ENIT, University of Tunis El Manar, B.P. 37, 1002 Tunis, Tunisia

E-mail: habbal@unice.fr (A.Habbal), moez.kallel@enit.utm.tn (M.Kallel) and marwalouni@gmail.com (M.Ouni).

Abstract.

We introduce a new algorithm to solve the problem of detecting unknown cavities immersed in a stationary viscous fluid, using partial boundary measurements. The considered fluid obeys a steady Stokes regime, the cavities are inclusions and the boundary measurements are a single compatible pair of Dirichlet and Neumann data, available only on a partial accessible part of the whole boundary. This inverse inclusion Cauchy-Stokes problem is ill-posed for both the cavities and missing data reconstructions, and designing stable and efficient algorithms is not straightforward. We reformulate the problem as a three-player Nash game. Thanks to an identifiability result derived for the Cauchy-Stokes inclusion problem, it is enough to set up two Stokes BVP, then use them as state equations. The Nash game is then set between 3 players, the two first targeting the data completion while the third one targets the inclusion detection. We used a level-set approach to get rid of the tricky control dependence of functional spaces, and we provided the third player with the level-set function as strategy, with a cost functional of Kohn-Vogelius type. We propose an original algorithm, which we implemented using Freefem++. We present 2D numerical experiments for three different test-cases. The obtained results corroborate the efficiency of our 3-player Nash game approach to solve parameter or shape identification for Cauchy problems.

Keywords: Data completion, Cauchy-Stokes problem, shape identification, Nash games.

Mathematics Subject Classifications (2010): 49J20, 65K10, 65N06, 90C30

1. Introduction

Fluid dynamics are central in many industrial, biological and biomedical processes. The good functioning of the involved systems could be dramatically damaged in the presence of undesired small obstacles (impurities) or inclusions (cavitation). For example, polymer material degradation is related to the formation of inclusions during polymer extrusion [1]; as well, the mechanism of joint cracking is related to cavity formation [2].

A large spectrum of the processes above can be considered as Stokes flows, though they should be taken unsteady and anisotropic to render satisfactorily the complex phenomenon of the formation of cavities [3]. The shape and location of the inclusions is generally out of reach for direct observation, hence the need for effective nondestructive monitoring solutions, known as geometric inverse problems when mathematics and algorithms are involved. Popular mathematical models build on the assumption that some specific measurements are available over the whole boundary of the structure under investigation, dealing with partial differential equations of boundary value -BVP- type. However, it should be noticed that from a technological point of view, when industrial devices are involved, the assumption above is in general impossible to fulfill, either because it is too expensive, or simply because part of the boundary is not accessible to probing, think of a heart valve [4]. Such restrictions lead to develop complex protocols like for the detection of flaws in metal melts in foundry industry [5]. Industrial solutions use in general protocols where emission and reception of the probing signals are set on the same location of the boundary. From a mathematical point of view, we have access to over specified boundary data (e.g. temperature and thermal flux) on the probing location, and no data elsewhere. Thus, we deal with partial differential equations, having access to over specified boundary data, and missing data to recover as well as unknown inclusions to detect. We are then in the framework of geometric inverse problems for the so called Cauchy-Stokes system. We shall restrict ourselves to the case of steady and Newtonian Stokes flows.

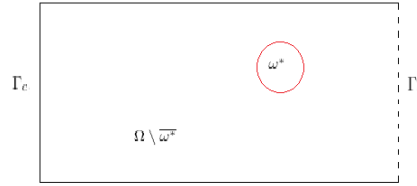


Figure 1: An example of the geometric configuration of the problem : the whole domain including cavities is denoted by Ω . It contains an inclusion ω^* . The boundary of Ω is composed of Γ_c , an accessible part where over-specified data are available, and an inaccessible part Γ_i where the data are missing.

1 Let us introduce a preliminary mathematical description of the problem. Consider a bounded open domain
 2 $\Omega \subset \mathbb{R}^d$ ($d=2, 3$) occupied by an incompressible viscous fluid, see Figure-1. We assume that the boundary $\partial\Omega$ is
 3 sufficiently smooth and composed of two connected components Γ_c and Γ_i . Let $\omega^* \subset\subset \Omega$ be an unknown inclusion
 4 immersed in Ω . The Cauchy-Stokes geometric inverse problem considered here consists, then, from given velocity
 5 f and fluid stress forces Φ prescribed only on the accessible part Γ_c of the boundary, to identify $\omega^* \in \mathcal{D}_{\text{ad}}$ (a set of
 6 admissible shapes defined later) such that the fluid velocity u and the pressure p are solution of the following Stokes
 7 problem:

$$8 \quad \left\{ \begin{array}{ll} \nu \Delta u - \nabla p = 0 & \text{in } \Omega \setminus \overline{\omega^*}, \\ \operatorname{div} u = 0 & \text{in } \Omega \setminus \overline{\omega^*}, \\ \sigma(u, p)n = 0 & \text{on } \partial\omega^*, \\ u = f & \text{on } \Gamma_c, \\ \sigma(u, p)n = \Phi & \text{on } \Gamma_c, \end{array} \right. \quad (1)$$

where n is the unit outward normal vector on the boundary, and $\sigma(u, p)$ the fluid stress tensor defined as follows:

$$\sigma(u, p) = -pI_d + 2\nu D(u)$$

9 with $D(u) = 1/2(\nabla u + \nabla u^T)$ being the linear strain tensor and I_d the identity matrix.
 10 For the sake of simplicity, from now on, the viscosity ν of the fluid is set to $\nu = 1$.

11
 12 Additionally to the geometric identification problem (i.e. detect the inclusions ω^*) one has to complete the bound-
 13 ary data, that is to recover the missing traces of the velocity u and of the normal stress $\sigma(u, p).n$ over Γ_i the inaccessible
 14 part of the boundary. Remark that the difference between obstacles and inclusions amounts to which boundary con-
 15 dition is used : homogeneous Dirichlet one for the obstacles and homogeneous Neumann condition for the inclusions
 16 (considered as free surfaces).

17
 18 Even when restricted to elliptic equations, mostly Laplace and Stokes systems, there exists a prolific literature
 19 dedicated to each of these two problems separately, and because of their well known ill-posedness (in the sense of
 20 Hadamard) [6], most of the literature addresses as well (if not exclusively) the ensuing stability and other computa-
 21 tional issues. For the Cauchy problem, far from being exhaustive, an excerpt of popular approaches are the least-square
 22 penalty techniques used in [7] and in the earlier paper [8], Tikhonov regularization methods [9], quasi reversibility
 23 methods [10], alternating iterative methods [11] [12] and control type methods andrieux2006solving [13]. Recently,
 24 an approach based on game theory, using decentralized strategies, was proposed in [14].

25
 26 Let us mention that many of the papers dedicated to data completion or to obstacle detection and based on control
 27 or optimization approaches, minimize a so-called Kohn-Vogelius type functional, an energy error function introduced
 28 in the framework of parameter identification in [15].

29
 30 Regarding the obstacle identification problem, a more challenging geometric inverse problem, and again with a
 31 very partial on the existing literature, the authors in [16] address the obstacle detection problem for unsteady Stokes

1 and Navier-Stokes flows, quasi reversibility coupled to a level set approach is used in [17] for the Laplace equation,
 2 shape optimization [18] and topological gradient [19] are used for the Stokes system, and in [20] stability issues are
 3 addressed for the inverse obstacle problem in a Stokes flow.

4
 5 In contrast, rather a few papers address the joint geometric and data completion inverse problems, at least re-
 6 garding its computational aspects. Close to our present work, the inverse obstacle problem for the Cauchy-Laplace
 7 equation is studied in [21] where a control-type approach is used and applied to a Kohn-Vogelius functional. In [22]
 8 the authors use quasi reversibility coupled to a level set approach to solve the inverse obstacle problem for the Cauchy-
 9 Stokes equations. A formulation based on nonlinear integral equations arising from the reciprocity gap[23] principle
 10 is used in [24].

11
 12 Presently, we consider the inverse inclusion problem for the Cauchy-Stokes system. In order to solve the joint
 13 completion/detection problem, we reformulate it as a three players Nash game, following the ideas introduced earlier
 14 in [14] to solve the Cauchy-Laplace (completion) problem.

15 The game is defined as follows: first, the Cauchy-Stokes problem is formulated as two boundary value problems
 16 (BVP). The first BVP defines the first player, it inherits the available Dirichlet data f specified on the boundary Γ_c , and
 17 has control on a Neumann data set over the inaccessible boundary Γ_i , the latter control being the first player's strategy
 18 aimed at minimizing the gap over Γ_c between first player's normal stress and the prescribed normal stress Φ . The
 19 second BVP defines the second player, as it inherits the available normal stress data Φ set over Γ_c , and uses Dirichlet
 20 data set over the inaccessible boundary Γ_i as strategy variables. The second player's Dirichlet strategy is aimed at
 21 minimizing the gap over Γ_c between second player's and the prescribed Dirichlet data f . The fading and regularizing
 22 difference between the solutions to these two BVPs is shared by the two players. The third player has no own BVP,
 23 but has access to the two previous ones, and uses as control variable the shape of the inclusion(s). The third player's
 24 criteria to minimize is a Kohn-Vogelius type functional. The three players play a static Nash game with complete
 25 information, whose relevant solution concept is the so-called Nash equilibrium (NE).

26 We shall present and prove some theoretical results for the Cauchy-Stokes problem, precisely that a Nash equi-
 27 librium exists and is unique, and coincides with the missing data as soon as the Cauchy problem has a solution (that is,
 28 when the over specified data are compatible). Then, we propose a new algorithm dedicated to the joint computation of
 29 the missing data and the obstacle shapes. In this algorithm, a Nash subgame is played by the completion first and sec-
 30 ond players in order to precondition the Cauchy problem and tackle its ill-posedness. A level set approach is used for
 31 the latter geometric identification problem. We lead a sensitivity analysis, and present several numerical experiments
 32 that corroborate the efficiency of our approach and its nice stability with respect to noisy data.

33
 34 The paper is organized as follows. In Section 2, we extend our previous [14] Nash game approach to the data
 35 completion for the steady Stokes flows. In view of the formulation of the geometric inverse problem, we first recall in
 36 Section 3 a now classical identifiability proof [16] usually established for obstacles, so with homogeneous Dirichlet
 37 boundary condition, with a minor adaption to fit the case of inclusions, whose boundary conditions are of homogeneous
 38 Neumann type. Then, we formulate in Section 4 the Nash game approach to tackle the joint completion and geometric
 39 identification problem. We detail our algorithm, and some numerical aspects of the level set method, used to capture
 40 the inclusion boundary. Section 5 is devoted to the presentation of three numerical 2D test cases which assess the
 41 ability of our algorithm to jointly recover the missing boundary data and the location and shape of the inclusions as
 42 well. We finally draw some concluding remarks in Section 6.

43 2. Data completion for the Stokes problem

44 We consider in the present section the case where possible obstacles or inclusions are known, which amounts to sim-
 45 ply not consider them, focusing solely on the data completion problem. In the following, we apply the Nash game
 46 formulation of [14] to the Stokes problem. Results and proofs in the cited reference extend easily to the present case.

47
 48 With the notations introduced previously, let be $f \in (H^{\frac{1}{2}}(\Gamma_c))^d$ and $\Phi \in (H^{-\frac{1}{2}}(\Gamma_c))^d$ given Cauchy data. The
 49 pressure field p being determined up to a constant, it is convenient to introduce the following space :

$$L_0^2(\Omega) = \{q \in L^2(\Omega) ; \int_{\Omega} q = 0\}.$$

1 The Cauchy-Stokes problem is stated as follows : find $u \in (H^1(\Omega))^d$ and $p \in L_0^2(\Omega)$ such that

$$2 \quad \left\{ \begin{array}{ll} \Delta u - \nabla p = 0 & \text{in } \Omega, \\ \operatorname{div} u = 0 & \text{in } \Omega, \\ u = f & \text{over } \Gamma_c, \\ \sigma(u, p)n = \Phi & \text{over } \Gamma_c, \end{array} \right.$$

3 The data completion problem, which is simply a reformulation of the Cauchy-Stokes one, amounts to find
4 $\tau^* \in (H^{\frac{1}{2}}(\Gamma_i))^d$ and $\eta^* \in (H^{-\frac{1}{2}}(\Gamma_i))^d$ such that $u = \tau^*$ and $\sigma(u, p)n = \eta^*$ over Γ_i .

5
6 For any given $\eta \in (H^{-\frac{1}{2}}(\Gamma_i))^d$ and $\tau \in (H^{\frac{1}{2}}(\Gamma_i))^d$, we define the states $(u_1(\eta), p_1(\eta)) \in (H^1(\Omega))^d \times L_0^2(\Omega)$ and
7 $(u_2(\tau), p_2(\tau)) \in (H^1(\Omega))^d \times L_0^2(\Omega)$ as the unique weak solutions of the following Stokes boundary value problems
8 (SP_1) and (SP_2) :

$$(SP_1) \quad \left\{ \begin{array}{ll} \Delta u_1 - \nabla p_1 = 0 & \text{in } \Omega, \\ \operatorname{div} u_1 = 0 & \text{in } \Omega, \\ u_1 = f & \text{on } \Gamma_c, \\ \sigma(u_1, p_1)n = \eta & \text{on } \Gamma_i, \end{array} \right. \quad (SP_2) \quad \left\{ \begin{array}{ll} \Delta u_2 - \nabla p_2 = 0 & \text{in } \Omega, \\ \operatorname{div} u_2 = 0 & \text{in } \Omega, \\ u_2 = \tau & \text{on } \Gamma_i, \\ \sigma(u_2, p_2)n = \Phi & \text{on } \Gamma_c. \end{array} \right.$$

9 We then define the following cost functionals :

$$10 \quad \mathcal{J}_1(\eta, \tau) = \frac{1}{2} \|\sigma(u_1(\eta), p_1(\eta))n - \Phi\|_{(H^{-\frac{1}{2}}(\Gamma_c))^d}^2 + \frac{1}{2} \|u_1(\eta) - u_2(\tau)\|_{(H^{\frac{1}{2}}(\Gamma_i))^d}^2 \quad (2)$$

$$11 \quad \mathcal{J}_2(\eta, \tau) = \frac{1}{2} \|u_2(\tau) - f\|_{(H^{\frac{1}{2}}(\Gamma_c))^d}^2 + \frac{1}{2} \|u_1(\eta) - u_2(\tau)\|_{(H^{\frac{1}{2}}(\Gamma_i))^d}^2 \quad (3)$$

12 We are now in a position to formulate the two-player Nash game. The first player is defined by its strategy
13 $\eta \in (H^{-\frac{1}{2}}(\Gamma_i))^d$ and cost \mathcal{J}_1 , while the second one has control on $\tau \in (H^{\frac{1}{2}}(\Gamma_i))^d$ and aims at minimizing the cost
14 \mathcal{J}_2 . The two players play a static Nash game with complete information. The most popular solution concept for such
15 games is the one of a Nash equilibrium (NE) given by the

16 **Definition 1** A strategy pair $(\eta_N, \tau_N) \in (H^{-\frac{1}{2}}(\Gamma_i))^d \times (H^{\frac{1}{2}}(\Gamma_i))^d$ is a Nash equilibrium if the following holds:

$$17 \quad \left\{ \begin{array}{l} \mathcal{J}_1(\eta_N, \tau_N) \leq \mathcal{J}_1(\eta, \tau_N), \quad \forall \eta \in (H^{-\frac{1}{2}}(\Gamma_i))^d, \\ \mathcal{J}_2(\eta_N, \tau_N) \leq \mathcal{J}_2(\eta_N, \tau), \quad \forall \tau \in (H^{\frac{1}{2}}(\Gamma_i))^d. \end{array} \right. \quad (4)$$

18 The recourse to a game formulation and to a NE solution finds its justification in the following result :

19 **Proposition 1** Consider the Nash game defined above, with costs given by (2) and (3).

20 (i) There always exists a unique Nash equilibrium $(\eta_N, \tau_N) \in (H^{-\frac{1}{2}}(\Gamma_i))^d \times (H^{\frac{1}{2}}(\Gamma_i))^d$, which is also the minimum of the potential

$$L(\eta, \tau) = \frac{1}{2} \|\sigma(u_1(\eta), p_1(\eta))n - \Phi\|_{(H^{-\frac{1}{2}}(\Gamma_c))^d}^2 + \frac{1}{2} \|u_2(\tau) - f\|_{(H^{\frac{1}{2}}(\Gamma_c))^d}^2 + \frac{1}{2} \|u_1(\eta) - \tau\|_{(H^{\frac{1}{2}}(\Gamma_i))^d}^2.$$

21 (ii) If the Cauchy problem has a solution (u, p) , then $(u_1(\eta_N), p_1(\eta_N)) = (u_2(\tau_N), p_2(\tau_N)) = (u, p)$ and
22 (η_N, τ_N) are the missing data, i.e. $\eta_N = \sigma(u, p)n|_{\Gamma_i}$ and $\tau_N = u|_{\Gamma_i}$.

23 *Proof of (i).* We first prove the uniqueness of a NE. It is easy to check that the potential L is strictly convex by
24 computing its second order differential with respect to (η, τ) , see [13]. Thus, L has at most a one minimum. Moreover,

1 if it exists, the minimum of L is a Nash equilibrium, and conversely. Indeed, let be (η_0, τ_0) the minimum of L , then,
2 we have

$$3 \quad \begin{cases} L(\eta_0, \tau_0) \leq L(\eta, \tau_0), & \forall \eta \in (H^{-\frac{1}{2}}(\Gamma_i))^d, \\ L(\eta_0, \tau_0) \leq L(\eta_0, \tau), & \forall \tau \in (H^{\frac{1}{2}}(\Gamma_i))^d. \end{cases}$$

4 Thanks to the specific structure of L , this is equivalent to write

$$5 \quad \begin{cases} \mathcal{J}_1(\eta_0, \tau_0) \leq \mathcal{J}_1(\eta, \tau_0), & \forall \eta \in (H^{-\frac{1}{2}}(\Gamma_i))^d, \\ \mathcal{J}_2(\eta_0, \tau_0) \leq \mathcal{J}_2(\eta_0, \tau), & \forall \tau \in (H^{\frac{1}{2}}(\Gamma_i))^d. \end{cases}$$

6 That is, (η_0, τ_0) is a Nash equilibrium. Conversely, if (η_0, τ_0) is a Nash equilibrium then,

$$7 \quad \begin{cases} \mathcal{J}_1(\eta_0, \tau_0) \leq \mathcal{J}_1(\eta, \tau_0), & \forall \eta \in (H^{-\frac{1}{2}}(\Gamma_i))^d, \\ \mathcal{J}_2(\eta_0, \tau_0) \leq \mathcal{J}_2(\eta_0, \tau), & \forall \tau \in (H^{\frac{1}{2}}(\Gamma_i))^d. \end{cases}$$

8 Adding the term $\frac{1}{2} \|u_2(\tau) - f\|_{(H^{\frac{1}{2}}(\Gamma_c))^d}^2$ in the first inequality and the term $\frac{1}{2} \|\sigma(u_1, p_1)n - \Phi\|_{(H^{-\frac{1}{2}}(\Gamma_c))^d}^2$ in the
9 second one, we get,

$$10 \quad \begin{cases} L(\eta_0, \tau_0) \leq L(\eta, \tau_0), & \forall \eta \in (H^{-\frac{1}{2}}(\Gamma_i))^d, \\ L(\eta_0, \tau_0) \leq L(\eta_0, \tau), & \forall \tau \in (H^{\frac{1}{2}}(\Gamma_i))^d. \end{cases}$$

11 By the optimality conditions, we have

$$12 \quad \begin{cases} \frac{\partial L}{\partial \eta}(\eta_0, \tau_0) = 0, \\ \frac{\partial L}{\partial \tau}(\eta_0, \tau_0) = 0, \end{cases}$$

13 thus, (η_0, τ_0) is the minimum of L , the uniqueness of which implies that of the Nash equilibrium.

14 The proof of existence follows the same lines as in [14], the main ingredient being the uniform ellipticity of the
15 convex partial maps $\eta \rightarrow \mathcal{J}_1(\eta, \tau)$ and of $\tau \rightarrow \mathcal{J}_2(\eta, \tau)$ which allows for a direct application of the Nash Theorem,
16 see *ibidem* references to the Nash games and theorem.

17
18
19 *Proof of (ii).* If we assume that the Cauchy-Stokes problem has a solution (u, p) , which is then unique by the Holmgren
20 theorem, then let us define the following $\eta_C = \sigma(u, p)n|_{\Gamma_i}$ and $\tau_C = u|_{\Gamma_i}$. It is then straightforward to check that the
21 solutions $(u_1(\eta_C), p_1(\eta_C))$ to (SP_1) and $(u_2(\tau_C), p_2(\tau_C))$ to (SP_2) coincide with the Cauchy solution (u, p) , thanks
22 to the uniqueness of the solution of the boundary value Stokes problem. Thus, $L(\eta_C, \tau_C) = 0$ so that (η_C, τ_C) is a
23 minimum of $L \geq 0$. Thanks to the uniqueness result above, $(\eta_N, \tau_N) = (\eta_C, \tau_C)$.

For the computation of the NE for the Cauchy-Stokes problem, we used a popular algorithm [25] which amounts
basically to solve iteratively the following coupled problem, using gradient descent methods,

$$\begin{aligned} (\eta_N, \tau_N) &= \operatorname{argmin}_{\eta} \mathcal{J}_1(\eta, \tau_N), \\ (\eta_N, \tau_N) &= \operatorname{argmin}_{\tau} \mathcal{J}_2(\eta_N, \tau). \end{aligned}$$

24 We describe in Algorithm 1 below the main steps of the method, with a version where the Cauchy data of the
25 Dirichlet type f are possibly perturbed by a noise with some magnitude σ , yielding for the Cauchy problem a noisy
26 Dirichlet data f^σ :

Algorithm 1: Computation of a Cauchy-Stokes Nash equilibrium

Given : $\varepsilon > 0$ a convergence tolerance, Kmax a computational budget, σ a noise level and $\rho(\sigma)$ a -tuned- function which depends on the noise.

Choose an initial guess $S^{(0)} = (\eta^{(0)}, \tau^{(0)}) \in ((H^{-\frac{1}{2}}(\Gamma_c))^d \times (H^{\frac{1}{2}}(\Gamma_c))^d)$. Set $k = 1$.

- Step 1: Compute $\bar{\eta}^{(k)}$ solution of $\min_{\eta} \mathcal{J}_1(\eta, \tau^{(k-1)})$
and determine $\eta^{(k)} = t\eta^{(k-1)} + (1-t)\bar{\eta}^{(k)}$ with $0 \leq t < 1$.
- Step 2: Compute $\bar{\tau}^{(k)}$ solution of $\min_{\tau} \mathcal{J}_2(\eta^{(k-1)}, \tau)$
and determine $\tau^{(k)} = t\tau^{(k-1)} + (1-t)\bar{\tau}^{(k)}$ with $0 \leq t < 1$.
- Step 3: Compute $s_k = \|u_2^{(k)} - f^\sigma\|_{L^2(\Gamma_c)}$, where $(u_2^{(k)}, p_2^{(k)})$ is the solution of the following direct problem

$$\begin{cases} \Delta u_2^{(k)} - \nabla p_2^{(k)} = 0 & \text{in } \Omega, \\ \operatorname{div} u_2^{(k)} = 0 & \text{in } \Omega, \\ u_2^{(k)} = \tau^{(k)} & \text{on } \Gamma_i, \\ \sigma(u_2^{(k)}, p_2^{(k)})n = \Phi & \text{on } \Gamma_c. \end{cases}$$

While $s_k \geq \rho(\sigma)\varepsilon$ and $k < \text{Kmax}$ set $k = k + 1$, return back to step 1.

The gradient descent methods used to solve steps 1 and 2 in the algorithm above do require the computation of the gradients of the costs \mathcal{J}_1 and \mathcal{J}_2 , with respect to their respective strategies. The fast computation of the latter is classical, and led by means of an adjoint state method, as shown by the Proposition 2 below, see [13] for details.

We shall use the following classical notation :

$$H_\Gamma^1(\Omega) = \{\varphi \in (H^1(\Omega))^d \mid \varphi|_\Gamma = 0\} \text{ whenever } \Gamma \text{ is a non empty subset of the boundary of } \Omega.$$

Proposition 2 We have the following two partial derivatives:

$$(AP_1) \left\{ \begin{array}{l} \frac{\partial \mathcal{J}_1}{\partial \eta} \psi = - \int_{\Gamma} \psi \lambda_1 d\Gamma_i, \quad \forall \psi \in (H^{-\frac{1}{2}}(\Gamma_i))^d, \\ \text{with } (\lambda_1, \kappa_1) \in H_\Gamma^1(\Omega) \times L_0^2(\Omega) \text{ solution of the adjoint problem:} \\ \int_{\Gamma_c} (\sigma(u_1, p_1)n - \Phi)((\nabla \gamma + \nabla \gamma^T)n) d\Gamma_c + \int_{\Gamma} (u_1 - \tau)\gamma d\Gamma_i \\ + \int_{\Omega} (\nabla \gamma + \nabla \gamma^T) : \nabla \lambda_1 d\Omega - \int_{\Omega} \kappa_1 \operatorname{div} \gamma d\Omega = 0, \quad \forall \gamma \in H_\Gamma^1(\Omega). \\ - \int_{\Gamma_c} (\sigma(u_1, p_1)n - \Phi)\delta n d\Gamma_c - \int_{\Omega} \delta \operatorname{div} \lambda_1 d\Omega = 0, \quad \forall \delta \in L_0^2(\Omega), \end{array} \right.$$

$$(AP_2) \left\{ \begin{array}{l} \frac{\partial \mathcal{J}_2}{\partial \tau} \mu = \int_{\Gamma} (\sigma(\lambda_2, \kappa_2)n - (u_1(\eta) - u_2(\tau)))\mu d\Gamma_i, \quad \forall \mu \in (H^{\frac{1}{2}}(\Gamma_i))^d, \\ \text{with } (\lambda_2, \kappa_2) \in H_\Gamma^1(\Omega) \times L_0^2(\Omega) \text{ solution of the adjoint problem:} \\ \Delta \lambda_2 - \nabla \kappa_2 = 0 & \text{in } \Omega, \\ \operatorname{div} \lambda_2 = 0 & \text{in } \Omega, \\ \lambda_2 = 0 & \text{on } \Gamma_i, \\ \sigma(\lambda_2, \kappa_2)n = f - u_2(\tau) & \text{on } \Gamma_c, \end{array} \right.$$

where, by a classical convention, $\nabla u : \nabla v = \operatorname{Tr}(\nabla u \nabla v^T) = \sum_{i,j} \frac{\partial u_i}{\partial x_j} \frac{\partial v_i}{\partial x_j}$.

1 The existence and uniqueness of the solutions to the problems (AP_1) and (AP_2) , namely the adjoint states
 2 $(\lambda_1, \kappa_1) \in H_{\Gamma_c}^1(\Omega) \times L_0^2(\Omega)$ and $(\lambda_2, \kappa_2) \in (H^1(\Omega))^d \times L_0^2(\Omega)$ is straightforward, thanks to the regularity assumption
 3 on the Cauchy data $(f, \Phi) \in (H^{\frac{1}{2}}(\Gamma_c))^d \times (H^{-\frac{1}{2}}(\Gamma_c))^d$ and to regularity results on the solutions to the Stokes problems
 4 (SP_1) and (SP_2) , see e.g. [26] (or [27] Theorem 5.2).
 5

6 Later on, Algorithm 1 described above will be embedded into an overall algorithm with the specific task of
 7 processing the data recovery problem. We shall then use the partial derivatives given by Proposition 2. The overall
 8 algorithm stems from the Nash game played by the data recovery problem against the inclusion inverse problem. Next
 9 section is then devoted to a mandatory preamble for geometric inverse problems, that is the identifiability question.

10 3. An identifiability result for the inverse inclusion Cauchy-Stokes problem

11 In the present section, we adapt an identifiability result in [16], established for the case of obstacles, that is with a
 12 homogeneous Dirichlet condition, to the case of inclusions defined by Neumann (or free surface) boundary conditions.

The set of admissible inclusions is defined by :

$$\mathcal{D}_{\text{ad}} = \{\omega \subset\subset \Omega \text{ is open, Lipschitz and } \Omega \setminus \bar{\omega} \text{ is connected}\}.$$

13 We follow *grosso modo* the same proof technique of [16], noticing that, differently from the obstacle (Dirichlet)
 14 case, inclusions are not identifiable in case of over specified data f of affine free divergence form. Consequently, even
 15 if the over specified fluid stress Φ is identically zero, it is enough for the identifiability to hold, that the velocity data f
 16 be non affine.

17 **Theorem 1** *Let be $\Omega \subset \mathbb{R}^2$ an open bounded Lipschitz domain and Γ_c a non-empty open subset of the boundary $\partial\Omega$.
 18 Assume there exists a pair of compatible data $(f, \Phi) \in (H^{\frac{1}{2}}(\Gamma_c))^d \times (H^{-\frac{1}{2}}(\Gamma_c))^d$ for the Cauchy-Stokes problem, such
 19 that either $\Phi \neq 0$ or f is not the trace of an affine divergence free function.*

20 *Consider two admissible open sets ω_1 and ω_2 in \mathcal{D}_{ad} . For $i = 1, 2$, let be (u_i, p_i) the solutions to the following
 21 Cauchy-Stokes inclusion problem :*

$$22 \quad \left\{ \begin{array}{ll} \Delta u_i - \nabla p_i = 0 & \text{in } \Omega \setminus \bar{\omega}_i, \\ \operatorname{div} u_i = 0 & \text{in } \Omega \setminus \bar{\omega}_i, \\ \sigma(u_i, p_i)n = 0 & \text{on } \partial\omega_i, \\ u_i = f & \text{on } \Gamma_c, \\ \sigma(u_i, p_i)n = \Phi & \text{on } \Gamma_c. \end{array} \right. \quad (5)$$

23 *Then $\omega_1 = \omega_2$.*

24 *Proof.* Denote by $\omega = \omega_1 \cup \omega_2$ and define, over the set $\Omega \setminus \bar{\omega}$, $v = u_1 - u_2$ and $q = p_1 - p_2$, where (u_1, p_1) and
 25 (u_2, p_2) are the solutions to the system (5).

One sees that (v, q) satisfies

$$\left\{ \begin{array}{ll} \Delta v - \nabla q = 0 & \text{in } \Omega \setminus \bar{\omega}, \\ \operatorname{div} v = 0 & \text{in } \Omega \setminus \bar{\omega}, \\ v = 0 & \text{on } \Gamma_c, \\ \sigma(v, q)n = 0 & \text{on } \Gamma_c. \end{array} \right.$$

1 Thus, thanks to the Holmgren uniqueness theorem for the Stokes system, we have $v = 0$ and $q = 0$ in $\Omega \setminus \bar{\omega}$ and then
 2 $u_1 = u_2$ in $\Omega \setminus \bar{\omega}$.
 3

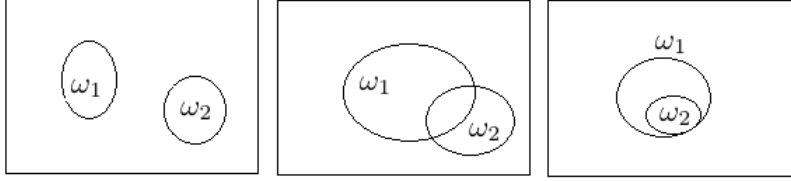


Figure 2: Different situations

4
 5 Let us suppose that $\omega_1 \neq \omega_2$, and assume then (up to a swap in subscripts) that $\omega_1 \setminus \bar{\omega}_2$ is an open non-empty subset
 6 of Ω . We know from system (5) that : $\Delta u_2 - \nabla p_2 = 0$ in $\omega_1 \setminus \bar{\omega}_2$.

7 We multiply the equation above by u_2 and take the integral over $\omega_1 \setminus \bar{\omega}_2$. Observe then that, thanks to $\operatorname{div} u_2 = 0$
 8 in $\omega_1 \setminus \bar{\omega}_2$, one has $\Delta u_2 = 2\operatorname{div}(D(u_2))$ where we recall that $D(u_2) = 1/2(\nabla u_2 + \nabla u_2^T)$.

By use of the Green formula, we obtain

$$\int_{\omega_1 \setminus \bar{\omega}_2} D(u_2) : \nabla u_2 dx - \int_{\omega_1 \setminus \bar{\omega}_2} p_2 \operatorname{div} u_2 dx = \int_{\partial(\omega_1 \setminus \bar{\omega}_2)} (-p_2 I_d + D(u_2)) n u_2 ds.$$

which can be rewritten as follows :

$$\frac{1}{2} \int_{\omega_1 \setminus \bar{\omega}_2} |D(u_2)|^2 dx = \int_{\partial(\omega_1 \setminus \bar{\omega}_2)} \sigma(u_2, p_2) n u_2 ds.$$

Now, since $\sigma(v, q)$ vanishes in $\Omega \setminus \bar{\omega}$, and thanks to the continuity of the involved -normal- traces, one has $\sigma(v, q)n = 0$
 on $\partial\omega$. From other part, one has $\sigma(u_1, p_1)n = 0$ on $\partial\omega_1$ thanks to equations (5). We then have $\sigma(u_2, p_2)n = 0$ on
 $\partial\omega_1 \setminus \partial(\omega_1 \cap \omega_2)$. Now, since we know that $\sigma(u_2, p_2)n = 0$ on $\partial\omega_2$ thanks to equations (5), we obtain

$$\int_{\partial(\omega_1 \setminus \bar{\omega}_2)} \sigma(u_2, p_2) n u_2 ds = 0,$$

that is,

$$\frac{1}{2} \int_{\omega_1 \setminus \bar{\omega}_2} |D(u_2)|^2 dx = 0.$$

9 Since $\|D(u_2)\|_{L^2(\omega_1 \setminus \bar{\omega}_2)}^2 = 0$, the components of the matrix of $D(u_2)$ are a.e. zero. Consequently, the velocity
 10 field u_2 has an affine form in $\omega_1 \setminus \bar{\omega}_2$, shortly given by $u_2(x) = Ax + b$ where A is a constant matrix with null diagonal.

We know from above and from equations (5) that (u_2, p_2) satisfies the following system,

$$\begin{cases} \Delta u_2 - \nabla p_2 = 0 & \text{in } \omega_1 \setminus \bar{\omega}_2, \\ \operatorname{div} u_2 = 0 & \text{in } \omega_1 \setminus \bar{\omega}_2, \\ \sigma(u_2, p_2)n = 0 & \text{on } \partial(\omega_1 \setminus \bar{\omega}_2). \end{cases}$$

11 Thus, by application (to $u_2(x) - (Ax + b)$ which fulfills the system above) of the unique continuation theorem for the
 12 steady Stokes equation established in [28], we conclude that $u_2(x) = Ax + b$ and $p_2 = 0$ in the whole domain $\Omega \setminus \bar{\omega}_2$.

1 Finally, reasoning with the traces on the boundary of the domain $\partial\Omega$, we observe that $u_2(x) = Ax + b$ and $p_2 = 0$
 2 in $\Omega \setminus \overline{\omega_2}$ yields $\sigma(u_2, p_2)n = \Phi = 0$ and $u_2(x) = f(x) = Ax + b$ over Γ_c , which, by assumption, is impossible. We
 3 conclude that $\omega_1 \setminus \overline{\omega_2} = \emptyset$, and so $\omega_1 = \omega_2$. ■

4 The identifiability result suggests that there is no need for a third party state equation, the two state equations
 5 (SP_1) and (SP_2) formulated with inclusions and dedicated to the completion problem should suffice. Only a
 6 third player's cost functional should be defined, playing with inclusions as strategies. Hence we enforced the data
 7 completion steps, by letting the first and second players lead a Nash subgame during the overall iterations, see next
 8 section. Numerical experiments show that this choice turned out to be efficient.

9 4. Coupled data completion and geometry identification for the Stokes problem

10 The aim of the present section is to introduce an algorithm dedicated to recover the missing boundary data while
 11 solving the inverse inclusion problem for steady Stokes flows. We extend the two-player Nash game set for the
 12 completion problem to a three-player Nash game, the third player being in charge of the inverse inclusion problem.

13 We recall that the inverse inclusion problem amounts to find $\omega^* \in \mathcal{D}_{\text{ad}}$ such that the fluid velocity u and the
 14 pressure p are solution to the following Cauchy-Stokes problem:

$$15 \quad \left\{ \begin{array}{ll} \Delta u - \nabla p = 0 & \text{in } \Omega \setminus \overline{\omega^*}, \\ \operatorname{div} u = 0 & \text{in } \Omega \setminus \overline{\omega^*}, \\ \sigma(u, p)n = 0 & \text{on } \partial\omega^*, \\ u = f & \text{on } \Gamma_c, \\ \sigma(u, p)n = \Phi & \text{on } \Gamma_c, \end{array} \right. \quad (6)$$

16 Thanks to the identifiability result stated in section 3, a single pair of -compatible- measurements (f, Φ) is enough
 17 to recover the inclusion(s) as well as the missing data. Next, we shall set up a three-player Nash game following the
 18 same philosophy than in section 2 dedicated for the sole completion.

19 For $\eta \in (H^{-\frac{1}{2}}(\Gamma_i))^d$, $\tau \in (H^{\frac{1}{2}}(\Gamma_i))^d$ and $\omega \in \mathcal{D}_{\text{ad}}$, let us define the following three cost functionals:

$$20 \quad \mathcal{J}_1(\eta, \tau; \omega) = \frac{1}{2} \|\sigma(u_1^\omega(\eta), p_1^\omega(\eta))n - \Phi\|_{(H^{-\frac{1}{2}}(\Gamma_c))^d}^2 + \frac{1}{2} \|u_1^\omega(\eta) - u_2^\omega(\tau)\|_{(H^{\frac{1}{2}}(\Gamma_i))^d}^2, \quad (7)$$

$$21 \quad \mathcal{J}_2(\eta, \tau; \omega) = \frac{1}{2} \|u_2^\omega(\tau) - f\|_{(H^{\frac{1}{2}}(\Gamma_c))^d}^2 + \frac{1}{2} \|u_1^\omega(\eta) - u_2^\omega(\tau)\|_{(H^{\frac{1}{2}}(\Gamma_i))^d}^2, \quad (8)$$

$$22 \quad \mathcal{J}_3(\eta, \tau; \omega) = \|\sigma(u_1^\omega(\eta), p_1^\omega(\eta)) - \sigma(u_2^\omega(\tau), p_2^\omega(\tau))\|_{L^2(\Omega \setminus \overline{\omega})^d}^2 + \mu |\partial\omega|, \quad (9)$$

where $(u_1^\omega(\eta), p_1^\omega(\eta))$ and $(u_2^\omega(\tau), p_2^\omega(\tau))$ are the solutions of the respective BVP (\mathcal{P}_1) and (\mathcal{P}_2) :

$$(\mathcal{P}_1) \quad \left\{ \begin{array}{ll} \Delta u_1^\omega - \nabla p_1^\omega = 0 & \text{in } \Omega \setminus \overline{\omega}, \\ \operatorname{div} u_1^\omega = 0 & \text{in } \Omega \setminus \overline{\omega}, \\ \sigma(u_1^\omega, p_1^\omega)n = 0 & \text{on } \partial\omega, \\ u_1^\omega = f & \text{on } \Gamma_c, \\ \sigma(u_1^\omega, p_1^\omega)n = \eta & \text{on } \Gamma_i, \end{array} \right. \quad (\mathcal{P}_2) \quad \left\{ \begin{array}{ll} \Delta u_2^\omega - \nabla p_2^\omega = 0 & \text{in } \Omega \setminus \overline{\omega}, \\ \operatorname{div} u_2^\omega = 0 & \text{in } \Omega \setminus \overline{\omega}, \\ \sigma(u_2^\omega, p_2^\omega)n = 0 & \text{on } \partial\omega, \\ \sigma(u_2^\omega, p_2^\omega)n = \Phi & \text{on } \Gamma_c, \\ u_2^\omega = \tau & \text{on } \Gamma_i. \end{array} \right.$$

1 In a few words, there are three players: Player (1) controls the strategy variable $\eta \in (H^{-\frac{1}{2}}(\Gamma_i))^d$ and aims at
 2 minimizing the cost \mathcal{J}_1 and Player (2) controls the strategy variable $\tau \in (H^{\frac{1}{2}}(\Gamma_i))^d$ and aims at minimizing the
 3 cost \mathcal{J}_2 . These two players may be interpreted exactly the same way than in the completion game stated section
 4 2: they are given Dirichlet (resp. Neumann) data and try to minimize the gap with the Neumann (resp. Dirichlet)
 5 remaining condition. The player (3) controls the strategy variable $\omega \in \mathcal{D}_{\text{ad}}$ and aims at minimizing the Kohn-Vogelius
 6 type functional \mathcal{J}_3 .

7 Notice that the state variables $(u_1^\omega(\eta), p_1^\omega(\eta))$ and $(u_2^\omega(\tau), p_2^\omega(\tau))$ belong to the space $(H^1(\Omega \setminus \bar{\omega}))^d \times L^2(\Omega \setminus \bar{\omega})$,
 8 which obviously depends on ω , a variable intended to be a control. In order to circumvent this tricky dependence, we
 9 recourse to a level-set formulation, before stating the actual three-player Nash game effectively implemented.

10 4.1. A level-set formulation

The level-set approach is a very convenient tool in shape identification, see [29] for a general introduction, or [30]
 where the approach is applied to detect obstacles in a Stokes flow. The boundary of the shape to be identified is
 postulated to be a zero level-set of a smooth enough (say Lipschitz) function $\phi : \Omega \rightarrow \mathbb{R}$. In other words, when ϕ
 varies in some -admissible- functional space, admissible open subsets $\omega \in \Omega$ are those defined by the following

$$\begin{cases} \phi(x) < 0 & \text{in } \omega, \\ \phi(x) > 0 & \text{in } \Omega \setminus \bar{\omega}, \\ \phi(x) = 0 & \text{on } \partial\omega. \end{cases}$$

11 The open set $\Omega \setminus \bar{\omega}$ is then given in terms of the level-set function as follows:

$$12 \quad \Omega \setminus \bar{\omega} = \{x \in \Omega \text{ such that } H(\phi(x)) = 1\}, \quad (10)$$

where $H(\cdot)$ is the Heaviside function. The perimeter of ω can then be formally given by

$$|\partial\omega| = \int_{\Omega} |\nabla H(\phi)| dx = \int_{\Omega} \delta(\phi) |\nabla \phi| dx.$$

13 where δ is the Dirac distribution.

14 For regularity reasons, and for ensuring the well-posedness of the modified Stokes system as well, it is usual to
 15 use smoothed versions of the Heaviside and Dirac distributions. Given two small enough parameters $\varepsilon > 0$ and $\beta > 0$,
 16 we used smoothed versions denoted respectively by $H_{\varepsilon, \beta}(\cdot)$ and $\delta_{\varepsilon, \beta}(\cdot)$, expressed as follows, for $s \in \mathbb{R}$,

$$17 \quad H_{\varepsilon, \beta}(s) = \begin{cases} 1 & \text{if } s > \varepsilon, \\ \frac{1}{2} \left(1 + \frac{2}{\pi} \arctan\left(\frac{s}{\varepsilon}\right) \right) & \text{if } |s| \leq \varepsilon, \\ \beta & \text{if } s < -\varepsilon, \end{cases} \quad \delta_{\varepsilon, \beta}(s) = \begin{cases} \frac{1}{\pi} \left(\frac{\varepsilon}{s^2 + \varepsilon^2} \right) & \text{if } |s| \leq \varepsilon, \\ \beta & \text{if } |s| > \varepsilon. \end{cases}$$

Let us now define the -control free- Sobolev state spaces : Given $g \in (H^{\frac{1}{2}}(\Gamma_c))^d$, $\psi \in (H^{\frac{1}{2}}(\Gamma_i))^d$

$$V_g = \{v \in H^1(\Omega)^d / \text{div} v = 0 \text{ and } v|_{\Gamma_c} = g\} \quad \text{and} \quad W_\psi = \{v \in H^1(\Omega)^d / \text{div} v = 0 \text{ and } v|_{\Gamma_i} = \psi\}.$$

18 Problems (\mathcal{P}_1) and (\mathcal{P}_2) are then rephrased in terms of the level-set, yielding the modified weak form :

$$(\mathcal{P}_{1, \varepsilon, \beta}) \begin{cases} \text{Find } (u_1^\phi, p_1^\phi) \in V_f \times L_0^2(\Omega) \text{ such that} \\ \int_{\Omega} (\sigma(u_1^\phi, p_1^\phi) : \nabla v_1) H_{\varepsilon, \beta}(\phi) d\Omega = \int_{\Gamma_i} \eta v_1 d\Gamma, \quad \forall v_1 \in H_{\Gamma_c}^1(\Omega), \end{cases} \quad (11)$$

$$(\mathcal{P}_{2_{\varepsilon,\beta}}) \begin{cases} \text{Find } (u_2^\phi, p_2^\phi) \in W_\tau \times L_0^2(\Omega) \text{ such that} \\ \int_\Omega (\sigma(u_2^\phi, p_2^\phi) : \nabla v_2) H_{\varepsilon,\beta}(\phi) d\Omega = \int_{\Gamma_c} \Phi v_2 d\Gamma, \quad \forall v_2 \in H_{\Gamma_c}^1(\Omega), \end{cases} \quad (12)$$

1 It is not the scope of the present paper to discuss the dependence of the modified Stokes problems with respect to
 2 (ε, β) , which is known to behave consistently [31] [32], so we still refer to problems $(\mathcal{P}_{1_{\varepsilon,\beta}})$ and $(\mathcal{P}_{2_{\varepsilon,\beta}})$ as (\mathcal{P}_1) and
 3 (\mathcal{P}_2) , and we omit to underline the dependence of the state variables w.r.t. (ε, β) as well.

4 4.2. Level-set sensitivity and optimality condition

The player (3) in charge of the inverse inclusion problem has now control on the level-set function ϕ instead of the open subset $\omega \in \mathcal{D}_{\text{ad}}$. The new form of the third player's cost functional is now as follows :

$$\mathcal{J}_3(\eta, \tau; \phi) = \int_\Omega |\sigma(u_2^\phi, p_2^\phi) - \sigma(u_1^\phi, p_1^\phi)|^2 H_{\varepsilon,\beta}(\phi) dx + \mu \int_\Omega \delta_{\varepsilon,\beta}(\phi) |\nabla \phi| dx$$

5 where (u_1^ϕ, p_1^ϕ) and (u_2^ϕ, p_2^ϕ) solve respectively problems (11) and (12). We choose as convenient space for the level-
 6 set variables the Sobolev space $\mathcal{S} = H^1(\Omega)$ though it is not optimal (in the sense that it may introduce too much
 7 regularity requirement, hampering the capture of non H^1 inclusions).

8 In order to perform the partial optimization of $\mathcal{J}_3(\eta, \tau; \phi)$ w.r.t. ϕ for (η, τ) given by players (1) and (2), one
 9 needs to compute the derivative of \mathcal{J}_3 w.r.t. ϕ . We have the following :

Proposition 3 *If $\phi \in \mathcal{S}$ satisfies the boundary condition $\frac{\partial \phi}{\partial n} = 0$ over $\partial\Omega$ then the partial derivative of $\mathcal{J}_3(\eta, \tau; \phi)$ with respect to ϕ , in any direction $\psi \in \mathcal{S}$, is given by*

$$\left(\frac{\partial \mathcal{J}_3}{\partial \phi}(\eta, \tau; \phi), \psi \right) = \int_\Omega \delta_{\varepsilon,\beta}(\phi) \left[|\sigma(u_2^\phi, p_2^\phi) - \sigma(u_1^\phi, p_1^\phi)|^2 - \mu \operatorname{div} \left(\frac{\nabla \phi}{|\nabla \phi|} \right) + \sigma(u_1^\phi, p_1^\phi) : \nabla \lambda_1 + \sigma(u_2^\phi, p_2^\phi) : \nabla \lambda_2 \right] \psi dx,$$

10 where $(\lambda_1, \pi_1) \in H_{\Gamma_c}^1(\Omega) \times L_0^2(\Omega)$ and $(\lambda_2, \pi_2) \in H_{\Gamma_c}^1(\Omega) \times L_0^2(\Omega)$ are respective solutions of the adjoints problems,

$$11 \left\{ \begin{array}{l} -2 \int_\Omega (\sigma(u_2^\phi, p_2^\phi) - \sigma(u_1^\phi, p_1^\phi)) : (\nabla h_1 + \nabla h_1^T) H_{\varepsilon,\beta}(\phi) - \int_\Omega (\operatorname{div} h_1) \pi_1 H_{\varepsilon,\beta}(\phi) \\ \quad + \int_\Omega ((\nabla h_1 + \nabla h_1^T) : \nabla \lambda_1) H_{\varepsilon,\beta}(\phi) = 0, \quad \forall h_1 \in H_{\Gamma_c}^1(\Omega), \\ 2 \int_\Omega (\sigma(u_2^\phi, p_2^\phi) - \sigma(u_1^\phi, p_1^\phi)) (k_1 I) H_{\varepsilon,\beta}(\phi) - \int_\Omega k_1 (\operatorname{div} \lambda_1) H_{\varepsilon,\beta}(\phi) = 0, \quad \forall k_1 \in L_0^2(\Omega), \end{array} \right. \quad (13)$$

$$12 \left\{ \begin{array}{l} 2 \int_\Omega (\sigma(u_2^\phi, p_2^\phi) - \sigma(u_1^\phi, p_1^\phi)) : (\nabla h_2 + \nabla h_2^T) H_{\varepsilon,\beta}(\phi) - \int_\Omega (\operatorname{div} h_2) \pi_2 H_{\varepsilon,\beta}(\phi) \\ \quad + \int_\Omega ((\nabla h_2 + \nabla h_2^T) : \nabla \lambda_2) H_{\varepsilon,\beta}(\phi) = 0, \quad \forall h_2 \in H_{\Gamma_c}^1(\Omega), \\ -2 \int_\Omega (\sigma(u_2^\phi, p_2^\phi) - \sigma(u_1^\phi, p_1^\phi)) (k_2 I) H_{\varepsilon,\beta}(\phi) - \int_\Omega k_2 (\operatorname{div} \lambda_2) H_{\varepsilon,\beta}(\phi) = 0, \quad \forall k_2 \in L_0^2(\Omega), \end{array} \right. \quad (14)$$

13 and where (u_1^ϕ, p_1^ϕ) and (u_2^ϕ, p_2^ϕ) are the solutions to respectively (11) and (12).

14 The proof of Proposition 3 above is given in Appendix.

1 The necessary optimality condition for the minimization problem $\min_{\phi \in \mathcal{S}} \mathcal{J}_3(\eta, \tau; \phi)$ is then formulated as the
 2 following Euler-Lagrange equation :

$$\begin{cases} \delta_{\varepsilon, \beta}(\phi) [|\sigma(u_2^\phi, p_2^\phi) - \sigma(u_1^\phi, p_1^\phi)|^2 - \mu \operatorname{div}(\frac{\nabla \phi}{|\nabla \phi|}) + \sigma(u_1^\phi, p_1^\phi) : \nabla \lambda_1 + \sigma(u_2^\phi, p_2^\phi) : \nabla \lambda_2] = 0, & \text{in } \Omega, \\ \frac{\partial \phi}{\partial n} = 0, & \text{on } \partial \Omega. \end{cases} \quad (15)$$

3 The strongly nonlinear equation above -with implicit terms- is solved iteratively as the stationary state of the
 4 following evolution equation

$$\begin{cases} \frac{\partial \phi}{\partial t} = -\delta_{\varepsilon, \beta}(\phi) [|\sigma(u_2^\phi, p_2^\phi) - \sigma(u_1^\phi, p_1^\phi)|^2 - \mu \operatorname{div}(\frac{\nabla \phi}{|\nabla \phi|}) + \sigma(u_1^\phi, p_1^\phi) : \nabla \lambda_1 + \sigma(u_2^\phi, p_2^\phi) : \nabla \lambda_2] = 0 & \text{in } \mathbb{R}^+ \times \Omega, \\ \frac{\partial \phi}{\partial n} = 0 & \text{on } \mathbb{R}^+ \times \partial \Omega, \\ \phi(0, x) = \phi_0(x) & \text{in } \Omega, \end{cases} \quad (16)$$

5 where $\phi_0 \in \mathcal{S}$ is a given initial condition.

6 The variational formulation associated to the problem (16) above reads

$$\begin{aligned} 7 \int_{\Omega} \frac{\partial \phi}{\partial t} \psi dx &= - \int_{\Omega} \delta_{\varepsilon, \beta}(\phi) \left[|\sigma(u_2^\phi, p_2^\phi) - \sigma(u_1^\phi, p_1^\phi)|^2 + \sigma(u_1^\phi, p_1^\phi) : \nabla \lambda_1 + \sigma(u_2^\phi, p_2^\phi) : \nabla \lambda_2 \right] \psi dx \\ &\quad + \int_{\Omega} \mu \delta_{\varepsilon, \beta}(\phi) \operatorname{div}(\frac{\nabla \phi}{|\nabla \phi|}) \psi dx, \quad \forall \psi \in H^1(\Omega). \end{aligned}$$

But, since one has

$$\operatorname{div}(\delta_{\varepsilon, \beta}(\phi) \frac{\nabla \phi}{|\nabla \phi|}) = \delta'_{\varepsilon, \beta}(\phi) \nabla \phi \frac{\nabla \phi}{|\nabla \phi|} + \delta_{\varepsilon, \beta}(\phi) \operatorname{div}(\frac{\nabla \phi}{|\nabla \phi|}),$$

8 we get,

$$\begin{aligned} 9 \int_{\Omega} \frac{\partial \phi}{\partial t} \psi dx &= - \int_{\Omega} \delta_{\varepsilon, \beta}(\phi) \left[|\sigma(u_2^\phi, p_2^\phi) - \sigma(u_1^\phi, p_1^\phi)|^2 + \sigma(u_1^\phi, p_1^\phi) : \nabla \lambda_1 + \sigma(u_2^\phi, p_2^\phi) : \nabla \lambda_2 \right] \psi dx \\ &\quad - \int_{\Omega} \frac{\mu \delta_{\varepsilon, \beta}(\phi)}{|\nabla \phi|} \nabla \phi \nabla \psi dx - \mu \int_{\Omega} \delta'_{\varepsilon, \beta}(\phi) |\nabla \phi| \psi dx, \quad \forall \psi \in H^1(\Omega). \end{aligned}$$

10 The problem above is solved numerically by means of a semi-implicit Euler scheme with $\frac{\partial \phi}{\partial t}$ approximated by
 11 $\frac{\phi^{n+1} - \phi^n}{\delta t}$, where $\phi^n(\cdot) = \phi(t_n, \cdot)$ and $t_n = n\delta t$, with $\delta t > 0$ a given time step.

12 We obtain the following iterative scheme:

$$\begin{cases} \text{Given } \phi^n, \text{ Find } \phi^{n+1} \in H^1(\Omega) \text{ such that:} \\ a(\phi^{n+1}, \psi) = l(\psi), \quad \forall \psi \in H^1(\Omega), \end{cases} \quad (17)$$

where

$$\begin{cases} a(\phi^{n+1}, \psi) = \int_{\Omega} \phi^{n+1} \psi dx + \delta t \int_{\Omega} \frac{\mu \delta_{\varepsilon, \beta}(\phi^n)}{|\nabla \phi^n|} \nabla \phi^{n+1} \nabla \psi dx, \\ l(\psi) = -\delta t \int_{\Omega} \delta_{\varepsilon, \beta}(\phi^n) \left[|\sigma(u_2^n, p_2^n) - \sigma(u_1^n, p_1^n)|^2 + \sigma(u_1^n, p_1^n) : \nabla \lambda_1^n + \sigma(u_2^n, p_2^n) : \nabla \lambda_2^n \right] \psi dx \\ \quad - \mu \delta t \int_{\Omega} \delta'_{\varepsilon, \beta}(\phi^n) |\nabla \phi^n| \psi dx + \int_{\Omega} \phi^n \psi dx \end{cases}$$

1

2 with $(u_1^n, p_1^n) = (u_1(\eta, \phi^n), p_1(\eta, \phi^n))$, $(u_2^n, p_2^n) = (u_2(\tau, \phi^n), p_2(\tau, \phi^n))$ are solutions to (11) and (12) for a given
3 ϕ^n , and $\lambda_{\{i=1,2\}}^n = \lambda_{\{i=1,2\}}(\phi^n)$ are the adjoint state solutions of the problems (13) and (14).

4

5 In order to prevent the level set iterates from being too flat or too steep, we trigger from time to time a
6 regularization pass that reinitializes the level set to a signed distance (see e.g. [33]). This step is mandatory in
7 order to keep the iterated level sets smooth enough, but is also necessary to have a non vanishing $|\nabla \phi^n|$ that ensures
the ellipticity of $a(\cdot, \cdot)$ in (17). The update is performed by solving the following equation :

$$\begin{cases} \frac{\partial \psi}{\partial t} + \text{sign}(\phi^n)(|\nabla \psi| - 1) = 0 & \text{in } \mathbb{R}^+ \times \Omega, \\ \frac{\partial \psi}{\partial n} = 0 & \text{on } \mathbb{R}^+ \times \partial\Omega, \\ \psi(0, x) = \phi^n(x) & \text{in } \Omega, \end{cases} \quad (18)$$

8

9 In practice, equation (18) above is solved for a few time steps (typically 5 or 6) then one reassigns the last
computed ψ to $\phi^n(x)$.

10

11 The six variational problems (11)–(14) (17) and (18) are solved by means of *ad hoc* Finite Element methods (see
Section 5 below).

12

4.3. The three-player Nash algorithm

13

14 We are now ready to state the three-player identification/completion Nash game. As aforementioned in section 4,
15 players (1) and (2) aim at solving the Cauchy problem, while player (3) is aimed at minimizing a Kohn-Vogelius type
16 energy, intended to capture the shape of the inclusion. The game is of Nash type, which means that it is static with
complete information [14] and hence its solution is a Nash equilibrium (NE), see Definition 4.

17

18 Given a triplet $(\eta, \tau, \phi) \in (H^{-\frac{1}{2}}(\Gamma_i))^d \times (H^{\frac{1}{2}}(\Gamma_i))^d \times \mathcal{S}$, let $(u_1^\phi(\eta), p_1^\phi(\eta))$ be the solution to the approximate
19 Stokes problem (11) and $(u_2^\phi(\tau), p_2^\phi(\tau))$ the solution to the approximate Stokes problem (12), then the three players
and their respective costs are defined as follows:

20

- Player (1) has control on the Neumann strategies $\eta \in (H^{-\frac{1}{2}}(\Gamma_i))^d$, and its cost functional is given by

21

$$\mathcal{J}_1(\eta, \tau, \phi) = \frac{1}{2} \|\sigma(u_1^\phi(\eta), p_1^\phi(\eta))n - \Phi\|_{(H^{-\frac{1}{2}}(\Gamma_c))^d}^2 + \frac{1}{2} \|u_1^\phi(\eta) - u_2^\phi(\tau)\|_{(H^{\frac{1}{2}}(\Gamma_i))^d}^2 \quad (19)$$

22

- Player (2) has control on the Dirichlet strategies $\tau \in (H^{\frac{1}{2}}(\Gamma_i))^d$, and its cost functional is given by

23

$$\mathcal{J}_2(\eta, \tau, \phi) = \frac{1}{2} \|u_2^\phi(\tau) - f\|_{(H^{\frac{1}{2}}(\Gamma_c))^d}^2 + \frac{1}{2} \|u_1^\phi(\eta) - u_2^\phi(\tau)\|_{(H^{\frac{1}{2}}(\Gamma_i))^d}^2 \quad (20)$$

24

- Player (3) has control on the inclusion level-set strategies $\phi \in \mathcal{S}$, and its cost functional is given by

25

$$\mathcal{J}_3(\eta, \tau; \phi) = \int_{\Omega} |\sigma(u_2^\phi(\tau), p_2^\phi(\tau)) - \sigma(u_1^\phi(\eta), p_1^\phi(\eta))|^2 H_{\varepsilon, \beta}(\phi) dx + \mu \int_{\Omega} \delta_{\varepsilon, \beta}(\phi) |\nabla \phi| dx \quad (21)$$

26

27 In Algorithm 2 below, we describe the main steps in computing the Nash equilibrium. This algorithm is unusual
28 in the sense that, first, it introduces a completion-oriented Nash subgame, solved incompletely (Kmax is small, around
29 ten iterations), and second, it processes the third player's minimization step by iterating on the necessary optimality
30 condition. Classical algorithms compute Nash equilibria with Kmax=1. It is easy to check (by writing down the
31 stationarity equations) that when the two algorithms converge, they lead to the same limit point, which is a Nash
equilibrium of the three-player's game defined above.

32

As we shall see in section 5 below, Algorithm 2 outperforms the classical one.

Algorithm 2: Computation of the coupled inclusion-completion Nash equilibrium

Given : convergence tolerances $\varepsilon_N > 0$, $\varepsilon_S > 0$, K_{\max} a computational budget per Nash iteration, N_{\max} a maximum Nash iterations, σ a noise level and $\rho(\sigma)$ a σ -tuned- function which depends on the noise.

Set $n = 0$, choose an initial level-set $\phi^{(0)} \in \mathcal{S}$.

- Step I: (a completion Nash subgame) Set $k = 1$.

Choose an initial guess $S^{(k-1)} = (\eta^{(k-1)}, \tau^{(k-1)}) \in ((H^{-\frac{1}{2}}(\Gamma_c))^d \times (H^{\frac{1}{2}}(\Gamma_c))^d)$.

- Step 1: Compute $\bar{\eta}^{(k)}$ solution of $\min_{\eta} \mathcal{J}_1(\eta, \tau^{(k-1)}, \phi^{(n)})$
and set $\eta^{(k)} = \alpha \eta^{(k-1)} + (1 - \alpha) \bar{\eta}^{(k)}$ with $0 \leq \alpha < 1$.

- Step 2: Compute $\bar{\tau}^{(k)}$ solution of $\min_{\tau} \mathcal{J}_2(\eta^{(k-1)}, \tau, \phi^{(n)})$
and set $\tau^{(k)} = \alpha \tau^{(k-1)} + (1 - \alpha) \bar{\tau}^{(k)}$ with $0 \leq \alpha < 1$.

- Step 3: While $\|S^{(k)} - S^{(k-1)}\| > \varepsilon_S$ and $k < K_{\max}$, set $k = k + 1$, return back to step 1.

- Step II: Compute $r_k = \|u_2^{(k)} - f^\sigma\|_{L^2(\Gamma_c)}$, where $(u_2^{(k)}, p_2^{(k)})$ is the solution of the problem (12) with the level-set $\phi = \phi^{(n)}$ and with the Dirichlet condition $u_2^{(k)} = \tau^{(k)}$ over Γ_i .

- Step III: While $r_k \geq \rho(\sigma)\varepsilon$ and $n < N_{\max}$ update the level-set : compute $\phi^{(n+1)}$ solution to the variational problem (17) and set $n = n + 1$, go back to step I.

5. Numerical experiments

In this section, we provide and discuss the numerical results of experiments led for three test cases, named A, B and C. These 3 test-cases share the following common settings :

The domain: $\Omega =]-\frac{1}{2}, \frac{1}{2}[\times]-\frac{1}{2}, \frac{1}{2}[$

The boundaries: $\Gamma_i = \{\frac{1}{2}\} \times]-\frac{1}{2}, \frac{1}{2}[$; $\Gamma_c = \partial\Omega \setminus \Gamma_i$

Normal stress: $\Phi(x, y) = -2(y^2 - 1/4; 0)$ prescribed over $\partial\Omega$

Initial strategies: for Step I, we always used $S^{(0)} = (\eta^{(0)}, \tau^{(0)}) = (0, 0)$ and took $\alpha = 0.10$

Parameters: for Step III : we took $\delta t = 0.02$ for solving equation (17).

The test-cases differ in the shape and/or number of connexe components of the inclusions.

Given a known shape and location of the inclusion $\omega^* \in \mathcal{D}_{\text{ad}}$, we solve the following Stokes problem :

$$\begin{cases} \Delta u - \nabla p = 0 & \text{in } \Omega \setminus \overline{\omega^*}, \\ \operatorname{div} u = 0 & \text{in } \Omega \setminus \overline{\omega^*}, \\ \sigma(u, p)n = 0 & \text{on } \partial\omega^*, \\ \sigma(u, p)n = \Phi & \text{on } \partial\Omega, \end{cases}$$

where the (phantom) exact solution (u, p) is used to build the remaining Cauchy data $f = u|_{\Gamma_c}$, and the exact missing data $u|_{\Gamma_i}$ and $\sigma(u, p)n|_{\Gamma_i}$. The two latter data together with the known inclusion shape ω^* are used to compute the following relative errors :

$$\begin{aligned} err_D &= \frac{\|\tau_N - u|_{\Gamma_i}\|_{L^2(\Gamma_i)}}{\|u|_{\Gamma_i}\|_{L^2(\Gamma_i)}}, & err_N &= \frac{\|\eta_N - \sigma(u, p)n|_{\Gamma_i}\|_{L^2(\Gamma_i)}}{\|\sigma(u, p)n|_{\Gamma_i}\|_{L^2(\Gamma_i)}}, \\ err_O &= \frac{mes(\omega^* \cup \omega_N) - mes(\omega^* \cap \omega_N)}{mes(\omega^*)}. \end{aligned} \tag{22}$$

1 where (η_N, τ_N, ϕ_N) is the approximate Nash equilibrium output from Algorithm 2, and $\omega_N = \mathbb{1}_{\{\phi_N < 0\}}$.
 2 These metrics are used to assess the efficiency of our approach. The stability w.r.t. noise was stressed by solving the
 3 joint inverse inclusion/completion problem with noisy perturbations of the Dirichlet data $f^\sigma = f + \sigma N$ with N being
 4 a Gaussian white noise.

5 Two different initial level-sets were used : $\phi_1^{(0)}$ has as zero level-set the disk $B(c_0, r_0)$ where $c_0 = (0, 0)$ and
 6 $r_0 = 0.30$, and $\phi_2^{(0)}$ is a periodic function with as zero level-set 30 fairly uniformly distributed small holes filling the
 7 whole domain Ω , see Figures 3(a) and 4(a).

8 The solvers for Stokes, equation (17) and adjoint systems, the sensitivity routines, and the minimization
 9 algorithms as well, were implemented using the Finite Element package FreeFem++ [34].

10 *Test-case A.*

11 The exact inclusion is a disk $\omega^* = B(c, r)$ centered at c and with a radius r where $c = (0, 0)$ and $r = 0.10$.

12 The FreeFem++ implementation of Algorithm 2 was ran for two different initial contours, leading to very close
 13 results, both of them in good accordance with the exact solutions (inclusion and missing data). It can be however
 14 observed from Figure 3(c)(e) and Figure 4(c)(e) that the initial contour $\phi_2^{(0)}$ outperforms $\phi_1^{(0)}$ as the computed first
 15 component of the fluid velocity and normal stress are more accurate with the initial contour $\phi_2^{(0)}$. Indeed, in all our
 16 subsequent numerical experiments, the initial contour $\phi_2^{(0)}$ outperformed $\phi_1^{(0)}$, so we shall later on present only those
 17 results obtained with $\phi_2^{(0)}$.

18 For the case of noisy Dirichlet data f^σ given over Γ_c , it can be seen from the profiles presented in Figure 5 that
 19 the boundary data recovery is remarkably stable with respect to the noise magnitude, and even more striking is the
 20 stability of the detected inclusion.

21 The relative errors defined by formulas (22) are summarized in Table 1 for the test-case A.

Noise level	$\sigma = 0\%$	$\sigma = 1\%$	$\sigma = 3\%$	$\sigma = 5\%$
err_D	0.010	0.015	0.039	0.063
err_N	0.031	0.033	0.051	0.07
err_O	0.032	0.043	0.066	0.117

Table 1: Test-case A. L^2 relative errors on missing data on Γ_i (on Dirichlet and Neumann data), and the error between the reconstructed and the real shape of the inclusion for various noise levels.

22 *Test-case B.*

The exact inclusion ω^* has a peanut-like shape, with a boundary parameterized as follows :

$$\partial\omega = \left\{ \left(\begin{array}{c} x_0 \\ y_0 \end{array} \right) + r(\theta) \left(\begin{array}{c} a \sin \theta \\ b \cos \theta \end{array} \right); \theta \in [0, 2\pi) \right\},$$

23 where $r(\theta) = \sqrt{\sin^2 \theta + 0.25 \cos^2 \theta}$, $(x_0, y_0) = (0, 0)$ and $(a, b) = (0.15, 0.18)$.
 24

25 In this test-case, the shape of the inclusion is nonconvex. We observe from Figure 6(b) that while the computed
 26 zero level-set is in good accordance with the exact one, it is however unable to accurately capture the nonconvex

1 features of the real inclusion. This is not very surprising in view of the different smoothed approximations used
 2 for the inclusion Stokes problems as well as for the level-set equation. The data completion results are however very
 3 satisfactory, as shown by the velocity and normal stress profiles in Figures 6(c)-(e). There is also a remarkable stability
 4 with respect to noisy data of both the inclusion detected and the recovered boundary data, see Figure 7.

5 *Test-case C.*

6 The inclusion to be detected is the union of two separate disks $\omega_1^* = B(c_1, r_1)$ centered at $c_1 = (0.2, 0.2)$ and with a
 7 radius $r_1 = 0.10$ and $\omega_2^* = B(c_2, r_2)$ centered at $c_2 = (-0.2, -0.2)$ and with a radius $r_2 = 0.12$.

8 This third and last test-case was set up to assess the ability of our algorithm to identify inclusions with several
 9 components. One observes from Figure 8(b) that the locations and the shapes of the two components of the inclusion
 10 are well detected, as well as the recovered data Figure 8(c)-(f). The recovery of missing boundary data is stable with
 11 respect to noisy Dirichlet measurements while there is a barely slight shift in the location of the detected approximation
 12 of ω_1^* for the noise levels 3% and 5%, as shown Figure 9.

13 The relative errors presented in Table 2 corroborate the stability of the detected contours and missing data with
 14 respect to noisy Dirichlet measurements.

Noise level	$\sigma = 0\%$	$\sigma = 1\%$	$\sigma = 3\%$	$\sigma = 5\%$
err_D	0.042	0.044	0.046	0.08
err_N	0.095	0.1	0.13	0.16
err_O	0.099	0.11	0.13	0.15

Table 2: Test-case C. L^2 -errors on missing data over Γ_i (on Dirichlet and Neumann data), and the error between the reconstructed and the real shape for various noise levels.

15 *Algorithm 2 vs Classical.*

16 In a classical algorithm [35] dedicated to the computation of a Nash equilibrium, there would be no preconditioning
 17 step as step I in Algorithm 2, or in other words, Kmax=1. We have compared these two approaches, for two noise
 18 free test-cases. We used the same number of total calls (400) to the Stokes Finite Element solvers. We see from Table
 19 3 that, for both test-cases, Algorithm 2 outperforms the classical one. The preconditioning Nash subgame in Step I,
 20 which is dedicated to enforce the data completion part does indeed enforce the identifiability property as well, since
 21 from the result established in Proposition 3, it is enough for a candidate velocity $u(\omega)$, for some inclusion ω , to be a
 22 Cauchy solution for the pair of boundary measurements (f, Φ) , to ensure that $\omega = \omega^*$, the real inclusion.

Case A	Classical algorithm	Algorithm 2	Case C	Classical algorithm	Algorithm 2
err_D	0.058	0.033	err_D	0.067	0.058
err_N	0.106	0.032	err_N	0.208	0.122
err_O	0.358	0.140	err_O	0.566	0.167

Table 3: Relative errors on the reconstructed missing data and inclusion shape for the Stokes problem (with noise free measurements), compared for a classical Nash algorithm and Algorithm 2 : (left) test-case A (right) test-case C.

6. Conclusion

We addressed in the present paper the delicate problem of detecting unknown cavities immersed in a stationary viscous fluid, using partial boundary measurements. The considered fluid obeys a Stokes regime, the cavities are inclusions and the boundary measurements are a single compatible pair of Dirichlet and Neumann data, available only on a partial accessible part of the whole boundary. This inverse inclusion Cauchy-Stokes problem is ill-posed for both the cavities and missing data reconstructions, and designing stable and efficient algorithms, which is the main goal of our work, is not straightforward.

The ill-posedness is tackled by decentralization : we reformulate it as a three players Nash game, following the ideas introduced earlier in [14] to solve the Cauchy-Laplace (completion) problem. Thanks to a simple yet strong identifiability result for the Cauchy-Stokes system, it is enough to set up two Stokes BVP, then use them as state equations. The Nash game is then set between 3 players, the two first targeting the data completion while the third one targets the inclusion detection. The latter problem is formulated using a level-set approach, and we provided the third player with the level-set function as strategy, while its cost functional is of Kohn-Vogelius type.

The class of algorithms we propose are summarized in Algorithm 2, the involved computational apparatus being rather classical : use of descent algorithms for the different minimizations, use of adjoint state method to compute the sensitivities, and use of Finite Element methods to solve the state and adjoint state equations, as well as to update the level-sets. We used Freefem++ to implement these routines.

We led 2D numerical experiments for three different test-cases. For noise free, as well as for noisy -Cauchy data- Dirichlet measurements, we obtained satisfactory results, exhibiting very stable behaviour with respect to the noise level (1%, 3%, 5%). The obtained results favor our 3-player Nash game approach to solve parameter or shape identification for Cauchy problems. Finally, our approach rises difficult theoretical questions that we did not address here, such as the existence, uniqueness and convergence issues for the level-set solution to the implicit optimality condition (15) and, related to the game-theoretic approach, the existence and convergence issues for the 3-player Nash equilibrium.

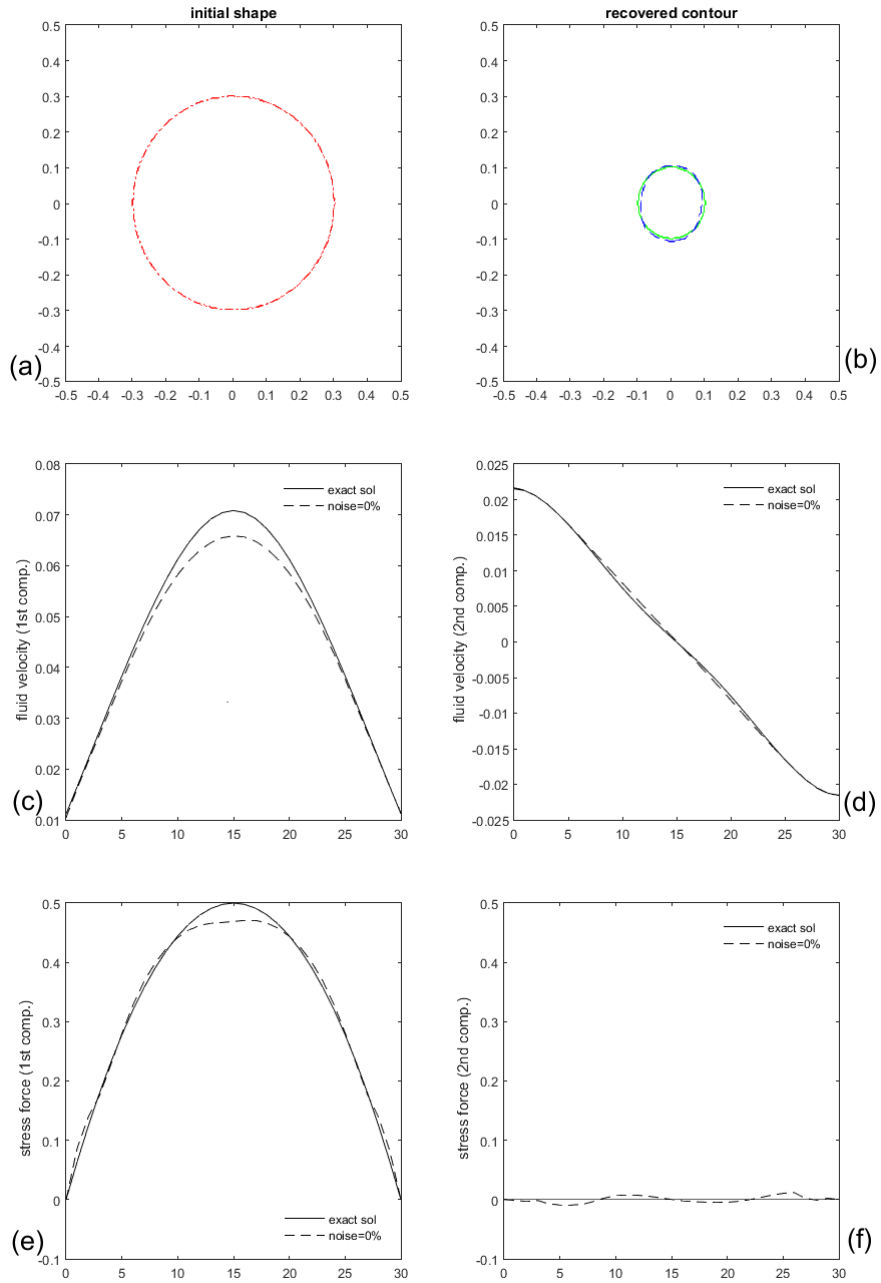


Figure 3: Test case A. Reconstruction of the inclusion shape and missing boundary data with noise free Dirichlet data over Γ_c . **(a)** initial contour is $\phi_1^{(0)}$ **(b)** exact inclusion shape -green line- and computed one - blue dashed- **(c)** exact -line- and computed -dashed line- first component of the velocity over Γ_i **(d)** exact -line- and computed -dashed line- second component of the velocity over Γ_i **(e)** exact -line- and computed -dashed line- first component of the normal stress over Γ_i **(f)** exact -line- and computed -dashed line- second component of the normal stress over Γ_i .

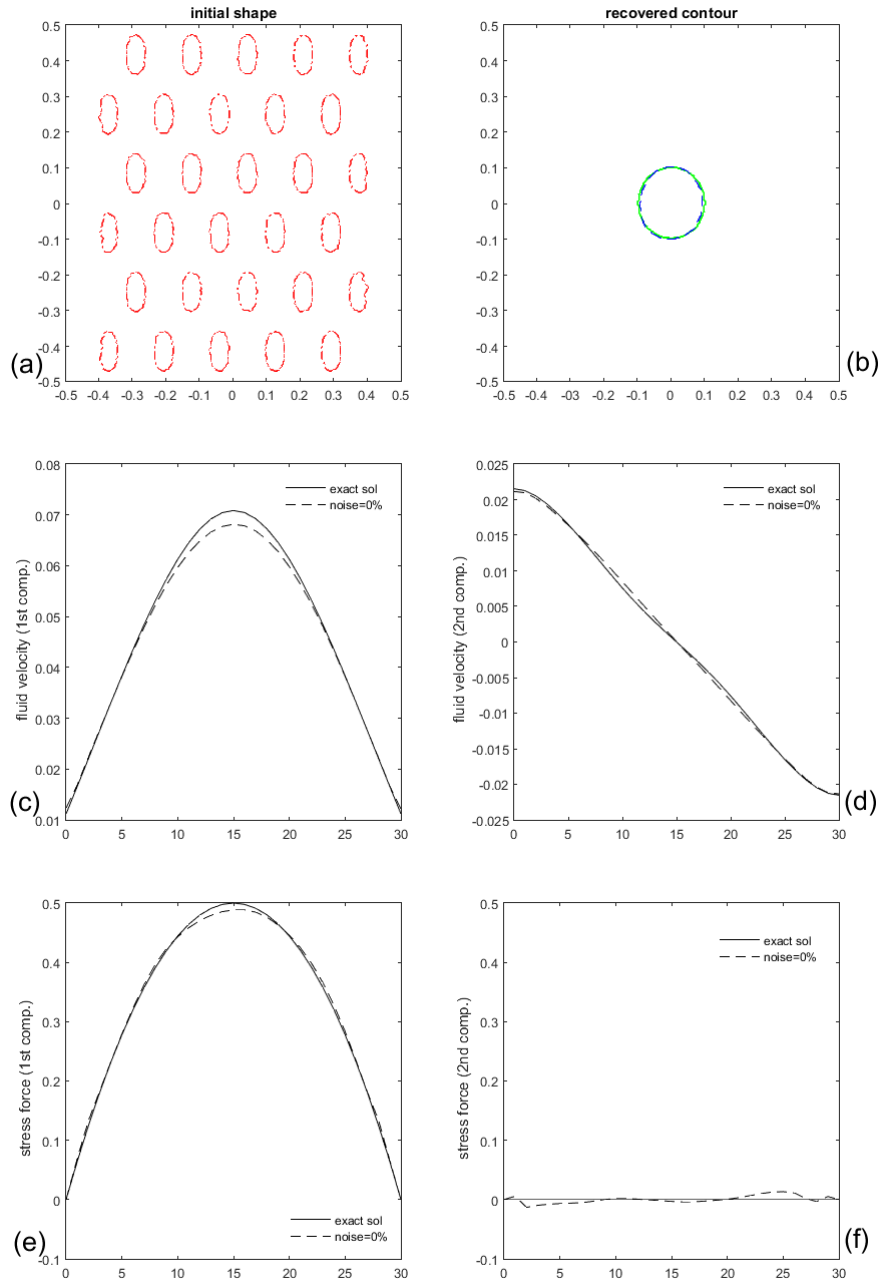


Figure 4: Test case A. Reconstruction of the inclusion shape and missing boundary data with noise free Dirichlet data over Γ_c . **(a)** initial contour is $\phi_2^{(0)}$ **(b)** exact inclusion shape -green line- and computed one - blue dashed- **(c)** exact -line- and computed -dashed line- first component of the velocity over Γ_i **(d)** exact -line- and computed -dashed line- second component of the velocity over Γ_i **(e)** exact -line- and computed -dashed line- first component of the normal stress over Γ_i **(f)** exact -line- and computed -dashed line- second component of the normal stress over Γ_i .

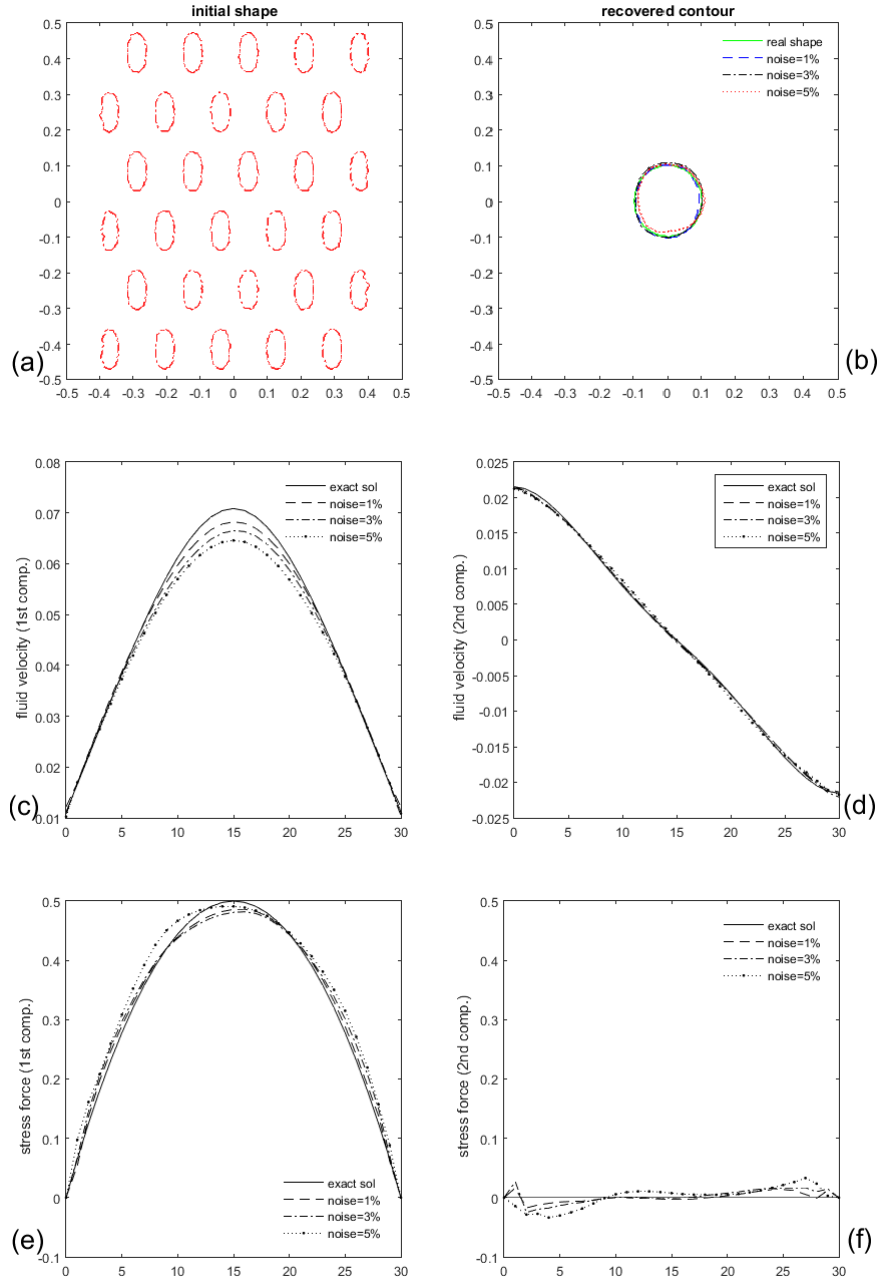


Figure 5: Test case A. Reconstruction of the inclusion shape and missing boundary data with noisy Dirichlet data over Γ_c with noise levels $\sigma = \{1\%, 3\%, 5\%\}$. (a) initial contour is $\phi_2^{(0)}$ (b) exact inclusion shape -green line- and computed ones for different noise levels (c) exact and computed first components of the velocity over Γ_i (d) exact and computed second components of the velocity over Γ_i (e) exact and computed first components of the normal stress over Γ_i (f) exact and computed second components of the normal stress over Γ_i .

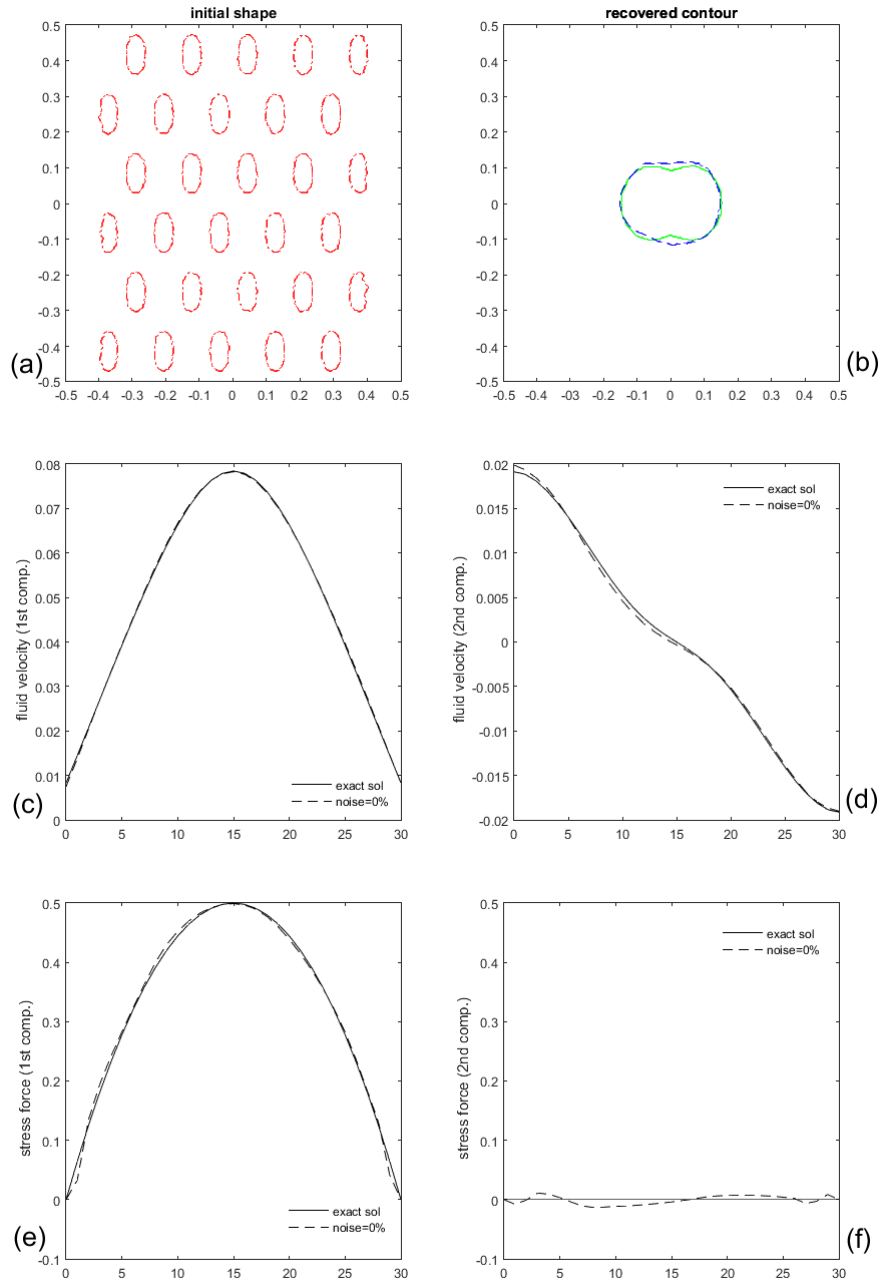


Figure 6: Test case B. Reconstruction of the inclusion shape and missing boundary data with noise free Dirichlet data over Γ_c . **(a)** initial contour is $\phi_2^{(0)}$ **(b)** exact inclusion shape -green line- and computed one - blue dashed- **(c)** exact -line- and computed -dashed line- first component of the velocity over Γ_i **(d)** exact -line- and computed -dashed line- second component of the velocity over Γ_i **(e)** exact -line- and computed -dashed line- first component of the normal stress over Γ_i **(f)** exact -line- and computed -dashed line- second component of the normal stress over Γ_i .

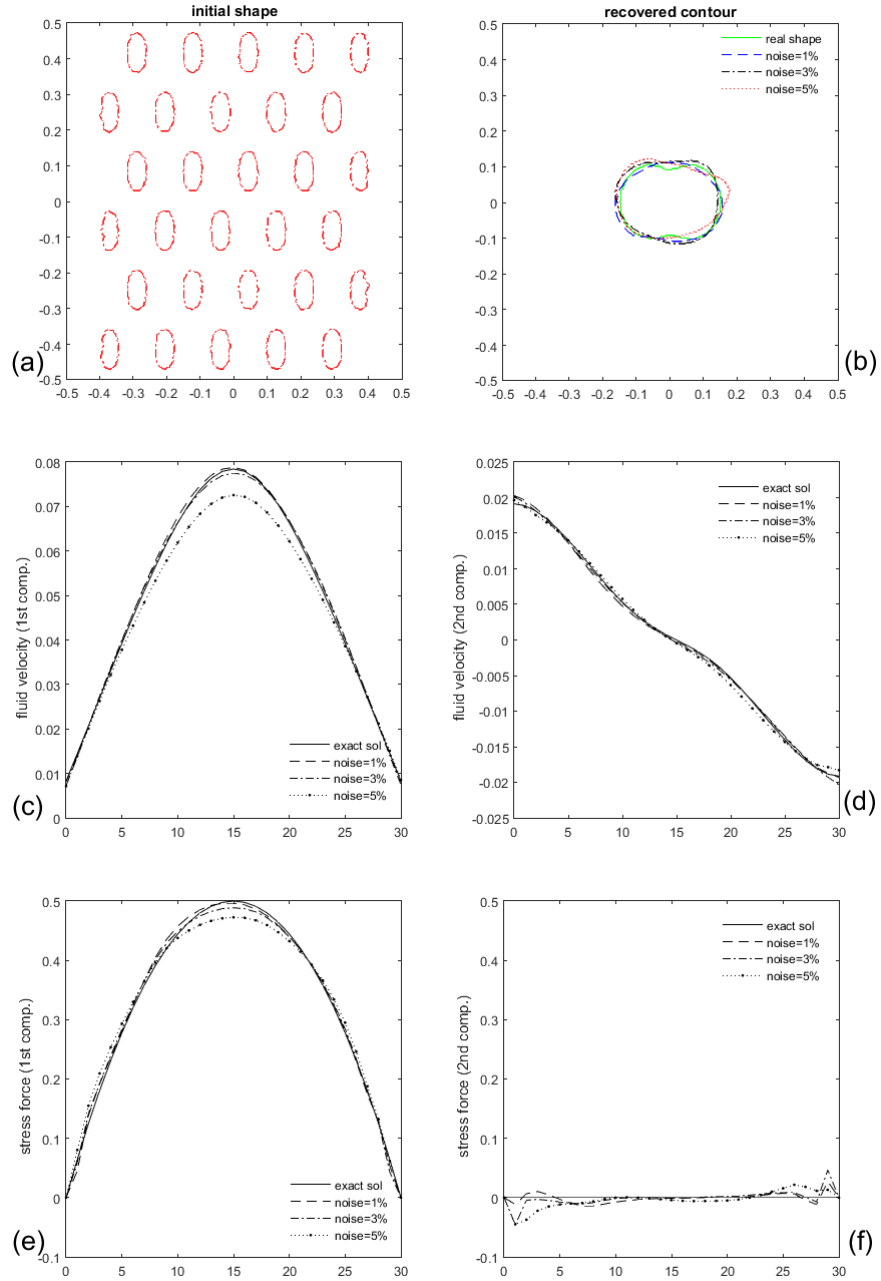


Figure 7: Test case B. Reconstruction of the inclusion shape and missing boundary data with noisy Dirichlet data over Γ_c with levels $\sigma = \{1\%, 3\%, 5\%\}$. **(a)** initial contour is $\phi_2^{(0)}$ **(b)** exact inclusion shape -green line- and computed ones for different noise levels **(c)** exact and computed first components of the velocity over Γ_i **(d)** exact and computed second components of the velocity over Γ_i **(e)** exact and computed first components of the normal stress over Γ_i **(f)** exact and computed second components of the normal stress over Γ_i .

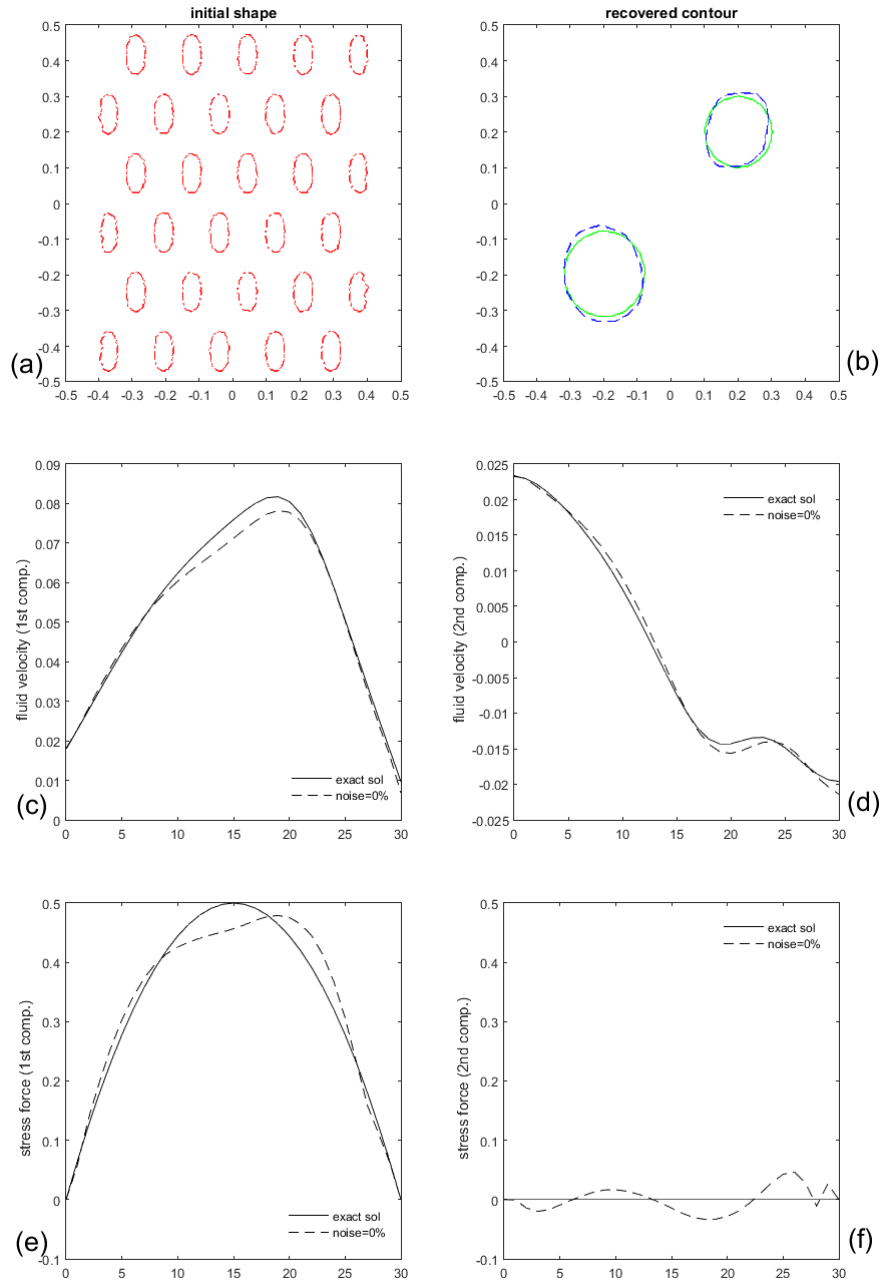


Figure 8: Test case C. Reconstruction of the inclusion shape and missing boundary data with noise free Dirichlet data over Γ_c . **(a)** initial contour is $\phi_2^{(0)}$ **(b)** exact inclusion shape -green line- and computed one - blue dashed- **(c)** exact -line- and computed -dashed line- first component of the velocity over Γ_i **(d)** exact -line- and computed -dashed line- second component of the velocity over Γ_i **(e)** exact -line- and computed -dashed line- first component of the normal stress over Γ_i **(f)** exact -line- and computed -dashed line- second component of the normal stress over Γ_i .

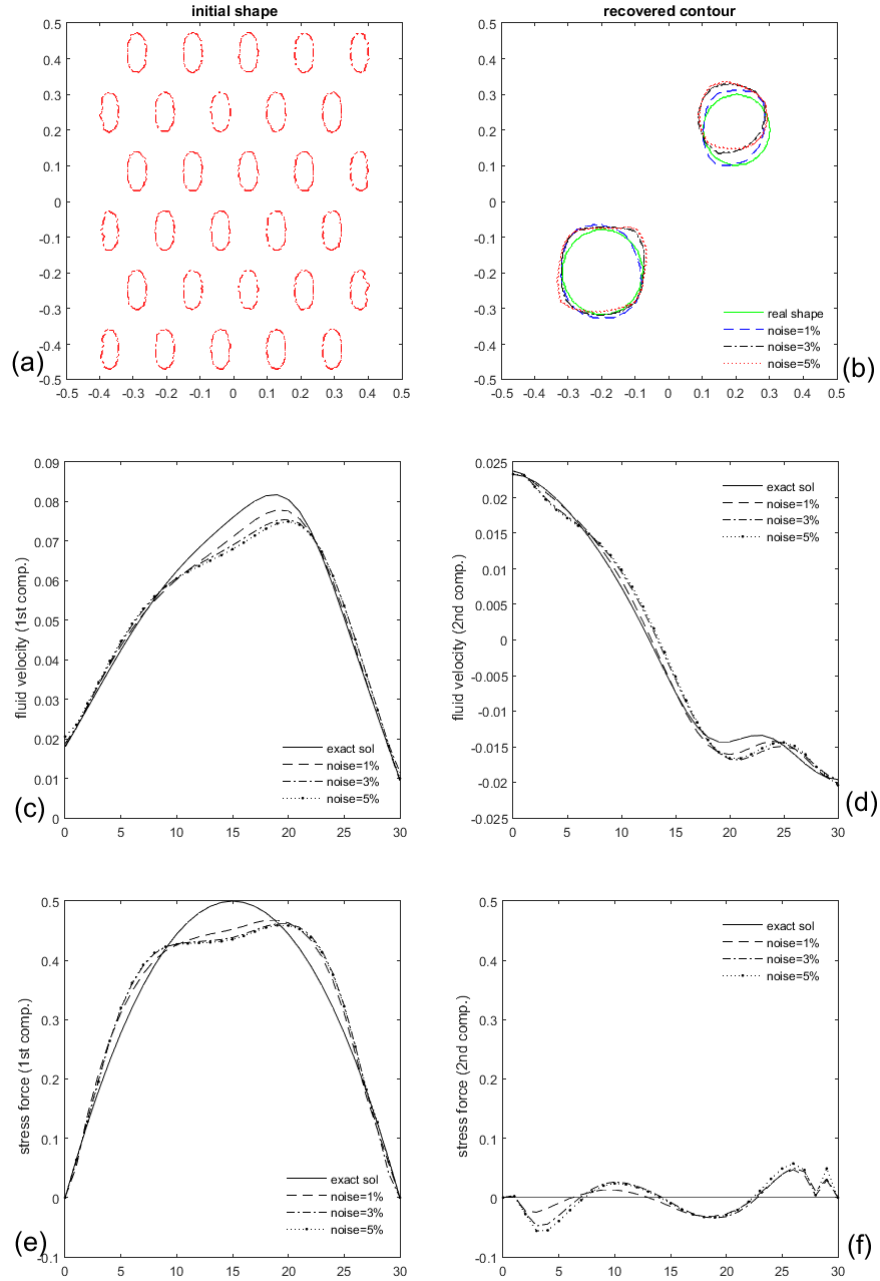


Figure 9: Test case C. Reconstruction of the inclusion shape and missing boundary data with noisy Dirichlet data over Γ_c with levels $\sigma = \{1\%, 3\%, 5\%\}$. **(a)** initial contour is $\phi_2^{(0)}$ **(b)** exact inclusion shape -green line- and computed ones for different noise levels **(c)** exact and computed first components of the velocity over Γ_i **(d)** exact and computed second components of the velocity over Γ_i **(e)** exact and computed first components of the normal stress over Γ_i **(f)** exact and computed second components of the normal stress over Γ_i .

1 **Appendix : proof of Proposition 3**

2 For fixed $(\eta, \tau) \in (H^{-\frac{1}{2}}(\Gamma_i))^d \times (H^{\frac{1}{2}}(\Gamma_i))^d$, let us define the Lagrangian \mathcal{L} by :

3

$$\begin{aligned} \mathcal{L}(\phi, \lambda_1, \pi_1, \lambda_2, \pi_2, u_1, p_1, u_2, p_2) &= \int_{\Omega} |\sigma(u_2, p_2) - \sigma(u_1, p_1)|^2 H_{\varepsilon, \beta}(\phi) dx + \mu \int_{\Omega} \delta_{\varepsilon, \beta}(\phi) |\nabla \phi| dx \\ &+ \int_{\Omega} (\sigma(u_1, p_1) : \nabla \lambda_1) H_{\varepsilon, \beta}(\phi) d\Omega - \int_{\Gamma_i} \eta \lambda_1 d\Gamma_i - \int_{\Omega} \pi_1 \operatorname{div} u_1 H_{\varepsilon, \beta}(\phi) d\Omega \\ &+ \int_{\Omega} (\sigma(u_2, p_2) : \nabla \lambda_2) H_{\varepsilon, \beta}(\phi) d\Omega - \int_{\Gamma_c} \Phi \lambda_2 d\Gamma_c - \int_{\Omega} \pi_2 \operatorname{div} u_2 H_{\varepsilon, \beta}(\phi) d\Omega, \end{aligned}$$

4

where the control $\phi \in \mathcal{S}$, the state variables $(u_1, u_2, p_1, p_2) \in V_f \times W_{\tau} \times L_0^2(\Omega) \times L_0^2(\Omega)$, the adjoint variables $(\lambda_1, \lambda_2) \in H_{\Gamma_c}^1(\Omega) \times H_{\Gamma_i}^1(\Omega)$ and $(\pi_1, \pi_2) \in L_0^2(\Omega) \times L_0^2(\Omega)$.

A formal derivation of the functional $\mathcal{J}_3(\eta, \tau; \phi)$ with respect to ϕ in some direction $\psi \in H^1(\Omega)$ yields

$$\begin{aligned} \frac{\partial \mathcal{J}_3}{\partial \phi}(\eta, \tau; \phi) \cdot \psi &= \int_{\Omega} |\sigma(u_2, p_2) - \sigma(u_1, p_1)|^2 \delta_{\varepsilon, \beta}(\phi) \psi + 2 \int_{\Omega} (\sigma(u_2, p_2) - \sigma(u_1, p_1)) (\sigma(u'_2, p'_2) - \sigma(u'_1, p'_1)) H_{\varepsilon, \beta}(\phi) \\ &+ \mu \int_{\Omega} \delta'_{\varepsilon, \beta}(\phi) |\nabla \phi| \psi + \mu \int_{\Omega} \delta_{\varepsilon, \beta}(\phi) \frac{\nabla \phi \nabla \psi}{|\nabla \phi|}, \quad \forall \psi \in H^1(\Omega), \end{aligned}$$

5 where we have used the notations $(u'_1, p'_1) = (\frac{\partial u_1}{\partial \phi} \psi, \frac{\partial p_1}{\partial \phi} \psi)$ and $(u'_2, p'_2) = (\frac{\partial u_2}{\partial \phi} \psi, \frac{\partial p_2}{\partial \phi} \psi)$.

6

7 We know that (u_1, p_1) solves the variational equation

8

$$\int_{\Omega} (\sigma(u_1, p_1) : \nabla v_1) H_{\varepsilon, \beta}(\phi) d\Omega = \int_{\Gamma_i} \eta v_1 d\Gamma_i, \quad \forall v_1 \in H_{\Gamma_c}^1(\Omega).$$

9 Then, (u'_1, p'_1) fulfills the following weak formulation

10

$$\int_{\Omega} (\sigma(u'_1, p'_1) : \nabla v_1) H_{\varepsilon, \beta}(\phi) d\Omega + \int_{\Omega} (\sigma(u_1, p_1) : \nabla v_1) \delta_{\varepsilon, \beta}(\phi) \psi d\Omega = 0, \quad \forall v_1 \in H_{\Gamma_c}^1(\Omega).$$

11 Now, we derive the Lagrangian \mathcal{L} with respect to u_1 and with respect to p_1 , we get

$$\left\{ \begin{array}{l} \frac{\partial \mathcal{L}}{\partial u_1} h_1 = -2 \int_{\Omega} (\nabla h_1 + \nabla h_1^T) : (\sigma(u_2, p_2) - \sigma(u_1, p_1)) H_{\varepsilon, \beta}(\phi) + \int_{\Omega} (\nabla h_1 + \nabla h_1^T) : \nabla \lambda_1 H_{\varepsilon, \beta}(\phi) \\ \quad - \int_{\Omega} \pi_1 \operatorname{div} h_1 = 0, \quad \forall h_1 \in H_{\Gamma_c}^1(\Omega), \\ \frac{\partial \mathcal{L}}{\partial p_1} k_1 = 2 \int_{\Omega} (k_1 I) : (\sigma(u_2, p_2) - \sigma(u_1, p_1)) H_{\varepsilon, \beta}(\phi) - \int_{\Omega} k_1 \operatorname{div}(\lambda_1) H_{\varepsilon, \beta}(\phi) \\ \quad = 0, \quad \forall k_1 \in L_0^2(\Omega). \end{array} \right. \quad (23)$$

12

13 If the pair (h_1, k_1) is replaced by (u'_1, p'_1) in (23) and because of $\operatorname{div} u_1 = 0$ implies $\operatorname{div} u'_1 = 0$, using the weak
14 formulation for the couple (u'_1, p'_1) , we get

15

$$-2 \int_{\Omega} (\sigma(u_2, p_2) - \sigma(u_1, p_1)) \sigma(u'_1, p'_1) H_{\varepsilon, \beta}(\phi) = \int_{\Omega} (\sigma(u_1, p_1) : \nabla \lambda_1) \delta_{\varepsilon, \beta}(\phi) \psi, \quad (24)$$

1 where (λ_1, π_1) solves the adjoint state problem

$$2 \left\{ \begin{array}{l} -2 \int_{\Omega} (\sigma(u_2, p_2) - \sigma(u_1, p_1)) : (\nabla h_1 + \nabla h_1^T) H_{\varepsilon, \beta}(\phi) - \int_{\Omega} \pi_1 \operatorname{div} h_1 H_{\varepsilon, \beta}(\phi) \\ \quad + \int_{\Omega} ((\nabla h_1 + \nabla h_1^T) : \nabla \lambda_1) H_{\varepsilon, \beta}(\phi) = 0, \quad \forall h_1 \in H_{\Gamma_1}^1(\Omega), \\ 2 \int_{\Omega} (\sigma(u_2, p_2) - \sigma(u_1, p_1)) (k_1 I) H_{\varepsilon, \beta}(\phi) - \int_{\Omega} k_1 \operatorname{div} \lambda_1 H_{\varepsilon, \beta}(\phi) = 0, \quad \forall k_1 \in L_0^2(\Omega). \end{array} \right.$$

3 In the same way, we find that

$$4 \quad 2 \int_{\Omega} (\sigma(u_2, p_2) - \sigma(u_1, p_1)) \sigma(u'_2, p'_2) H_{\varepsilon, \beta}(\phi) = \int_{\Omega} (\sigma(u_2, p_2) : \nabla \lambda_2) \delta_{\varepsilon, \beta}(\phi) \psi, \quad (25)$$

5 where (λ_2, π_2) solves the adjoint problem

$$6 \left\{ \begin{array}{l} 2 \int_{\Omega} (\sigma(u_2, p_2) - \sigma(u_1, p_1)) : (\nabla h_2 + \nabla h_2^T) H_{\varepsilon, \beta}(\phi) - \int_{\Omega} \pi_2 \operatorname{div} h_2 H_{\varepsilon, \beta}(\phi) \\ \quad + \int_{\Omega} ((\nabla h_2 + \nabla h_2^T) : \nabla \lambda_2) H_{\varepsilon, \beta}(\phi) = 0, \quad \forall h_2 \in H_{\Gamma_1}^1(\Omega), \\ -2 \int_{\Omega} (\sigma(u_2, p_2) - \sigma(u_1, p_1)) (k_2 I) H_{\varepsilon, \beta}(\phi) - \int_{\Omega} k_2 \operatorname{div} \lambda_2 H_{\varepsilon, \beta}(\phi) = 0, \quad \forall k_2 \in L_0^2(\Omega). \end{array} \right.$$

Using (24) and (25), we obtain

$$\frac{\partial \mathcal{J}_3}{\partial \phi}(\eta, \tau; \phi) \cdot \psi = \int_{\Omega} |\sigma(u_2, p_2) - \sigma(u_1, p_1)|^2 \delta_{\varepsilon, \beta}(\phi) \psi + \int_{\Omega} (\sigma(u_1, p_1) : \nabla \lambda_1) \delta_{\varepsilon, \beta}(\phi) \psi + \int_{\Omega} (\sigma(u_2, p_2) : \nabla \lambda_2) \delta_{\varepsilon, \beta}(\phi) \psi \\ + \mu \int_{\Omega} \delta'_{\varepsilon, \beta}(\phi) |\nabla \phi| \psi + \mu \int_{\Omega} \delta_{\varepsilon, \beta}(\phi) \frac{\nabla \phi \nabla \psi}{|\nabla \phi|}.$$

On the one hand, we have

$$\int_{\Omega} \operatorname{div}(\delta_{\varepsilon, \beta}(\phi) \frac{\nabla \phi}{|\nabla \phi|}) \psi dx = - \int_{\Omega} \delta_{\varepsilon, \beta}(\phi) \frac{\nabla \phi}{|\nabla \phi|} \nabla \psi dx + \int_{\partial \Omega} \frac{\delta_{\varepsilon, \beta}(\phi)}{|\nabla \phi|} \frac{\partial \phi}{\partial n} \psi ds,$$

and on the other hand,

$$\int_{\Omega} \operatorname{div}(\delta_{\varepsilon, \beta}(\phi) \frac{\nabla \phi}{|\nabla \phi|}) \psi dx = \int_{\Omega} \delta'_{\varepsilon, \beta}(\phi) |\nabla \phi| \psi dx + \int_{\Omega} \delta_{\varepsilon, \beta}(\phi) \operatorname{div}(\frac{\nabla \phi}{|\nabla \phi|}) \psi dx.$$

Then, if ϕ satisfies the boundary condition

$$\frac{\delta_{\varepsilon, \beta}(\phi)}{|\nabla \phi|} \frac{\partial \phi}{\partial n} = 0, \quad \text{on } \partial \Omega,$$

one can conclude that

$$\frac{\partial \mathcal{J}_3}{\partial \phi}(\eta, \tau; \phi) \cdot \psi = \int_{\Omega} |\sigma(u_2, p_2) - \sigma(u_1, p_1)|^2 \delta_{\varepsilon, \beta}(\phi) \psi + \int_{\Omega} (\sigma(u_1, p_1) : \nabla \lambda_1) \delta_{\varepsilon, \beta}(\phi) \psi + \int_{\Omega} (\sigma(u_2, p_2) : \nabla \lambda_2) \delta_{\varepsilon, \beta}(\phi) \psi \\ - \mu \int_{\Omega} \delta_{\varepsilon, \beta}(\phi) \operatorname{div}(\frac{\nabla \phi}{|\nabla \phi|}) \psi.$$

References

- [1] Younggon Son and Kalman B Migler. Cavitation of polyethylene during extrusion processing instabilities. *Journal of Polymer Science Part B: Polymer Physics*, 40(24):2791–2799, 2002.
- [2] Gregory N Kawchuk, Jerome Fryer, Jacob L Jaremko, Hongbo Zeng, Lindsay Rowe, and Richard Thompson. Real-time visualization of joint cavitation. *PLoS one*, 10(4):e0119470, 2015.
- [3] Tillmann Stieger, Hakam Agha, Martin Schoen, Marco G Mazza, and Anupam Sengupta. Hydrodynamic cavitation in stokes flow of anisotropic fluids. *Nature communications*, 8:15550, 2017.
- [4] Chi-Wen Lo, Sheng-Fu Chen, Chi-Pei Li, and Po-Chien Lu. Cavitation phenomena in mechanical heart valves: Studied by using a physical impinging rod system. *Annals of biomedical engineering*, 38(10):3162–3172, 2010.
- [5] Seymour Katz and Craig F Landefeld, editors. *On the Detection, Behaviour and Control of Inclusions in Liquid Metals*, pages 447–466. Springer US, Boston, MA, 1988.
- [6] J Hadamard. *The Cauchy Problem and the Linear Hyperbolic Partial Differential Equations*. Dover, New York, 1953.
- [7] RS Falk and PB Monk. Logarithmic convexity for discrete harmonic functions and the approximation of the cauchy problem for poisson’s equation. *Mathematics of computation*, 47(175):135–149, 1986.
- [8] P Colli Franzone and E Magenes. On the inverse potential problem of electrocardiology. *Calcolo*, 16(4):459–538, 1979.
- [9] A Cimetiere, F Delvare, M Jaoua, and F Pons. Solution of the cauchy problem using iterated tikhonov regularization. *Inverse problems*, 17(3):553, 2001.
- [10] Laurent Bourgeois. A mixed formulation of quasi-reversibility to solve the cauchy problem for laplace’s equation. *Inverse problems*, 21(3):1087, 2005.
- [11] V.A. Kozlov, V.G. Maz’ya, and A.V. Fomin. An iterative method for solving the cauchy problems for elliptic equations. *Comput. Math. Phys.*, 31:45–52, 1991.
- [12] T. Johansson and D. Lesnic. Reconstruction of a stationary flow from incomplete boundary data using iterative methods. *European Journal of Applied Mathematics*, 17:651–663, 2006.
- [13] A. Ben Abda R. Aboulaich and M. Kallel. A control type method for solving the cauchy-stokes problem. *Applied Mathematical Modelling*, 37:4295–4304, 2013.
- [14] A. Habbal and M. Kallel. Neumann-dirichlet nash strategies for the solution of elliptic cauchy problems. *SIAM Journal on Control and Optimization*, 51:4066–4083, 2013.
- [15] Robert V Kohn and Michael Vogelius. Relaxation of a variational method for impedance computed tomography. *Communications on Pure and Applied Mathematics*, 40(6):745–777, 1987.
- [16] C. Alvarez, C. Conca, L. Friz, O. Kaviani, and J. H. Ortega. Identification of immersed obstacles via boundary measurements. *Inverse Problems*, 21(5):1531–1552, 2005.
- [17] L. Bourgeois and J. Dardé. A quasi-reversibility approach to solve the inverse obstacle problem. *Inverse Probl. Imaging*, 4(3):351–377, 2010.
- [18] F. Caubet M. Badra and M. Dambrine. Detecting an obstacle immersed in a fluid by shape optimization methods. *Math. Models Methods Appl. Sci.*, 21(10):2069–2101, 2011.
- [19] C. Conca F. Caubet and M. Godoy. On the detection of several obstacles in 2d stokes flow : topological sensitivity and combination with shape derivatives. *Inverse Problems and Imaging*, 10:327–367, 2016.
- [20] A. Ballerini. Stable determination of an immersed body in a stationary stokes fluid. *Inverse Problems*, 26:125015(25pp), 2010.
- [21] Fabien Caubet, Jérémie Dardé, and Matias Godoy. On the data completion problem and the inverse obstacle problem with partial cauchy data for laplace’s equation. *ESAIM: Control, Optimisation and Calculus of Variations*, 2017.
- [22] Laurent Bourgeois and Jérémie Dardé. The exterior approach to solve the inverse obstacle problem for the stokes system. *Inverse Problems and Imaging*, 8(1):23–51, 2014.
- [23] S Andrieux and A Ben Abda. The reciprocity gap: a general concept for flaws identification problems. *Mechanics research communications*, 20(5):415–420, 1993.
- [24] CJS Alves, R Kress, and AL Silvestre. Integral equations for an inverse boundary value problem for the two-dimensional stokes equations. *Journal of Inverse and Ill-posed Problems jiiip*, 15(5):461–481, 2007.
- [25] H. Attouch, J. Bolte, and P. Redont. Alternating proximal algorithms for weakly coupled convex minimization problems. applications to dynamical games and pde’s. *J. Convex Anal.*, 15:485–506, 2008.
- [26] Giovanni Galdi. *An introduction to the mathematical theory of the Navier-Stokes equations: Steady-state problems*. Springer Science & Business Media, 2011.
- [27] G. Bastay, T. Johansson, V.A. Kozlov, and D. Lesnic. An alternating method for the stationary stokes system. *ZAMM*, 86:268–280, 2006.
- [28] C Fabre and G Lebeau. Unique continuation property of solutions of the stokes equation. *Communications in Partial Differential Equations*, 21(3-4):573–596, 1996.
- [29] Ravi Malladi, James A Sethian, and Baba C Vemuri. Shape modeling with front propagation: A level set approach. *IEEE transactions on pattern analysis and machine intelligence*, 17(2):158–175, 1995.
- [30] Fadil Santosa. A level-set approach for inverse problems involving obstacles. *ESAIM: Control, Optimisation and Calculus of Variations*, 1:17–33, 1996.
- [31] Xian-Bao Duan, Yi-Chen Ma, and Rui Zhang. Shape-topology optimization of stokes flow via variational level set method. *Applied Mathematics and Computation*, 202(1):200–209, 2008.
- [32] Mark Sussman, Peter Smereka, and Stanley Osher. A level set approach for computing solutions to incompressible two-phase flow. *Journal of Computational physics*, 114(1):146–159, 1994.
- [33] Grégoire Allaire, François Jouve, and Anca-Maria Toader. Structural optimization using sensitivity analysis and a level-set method. *Journal of computational physics*, 194(1):363–393, 2004.
- [34] F. Hecht. New development in freefem++. *J. Numer. Math.*, 20(3-4):251–265, 2012.
- [35] Shu Li and Tamer Başar. Distributed algorithms for the computation of noncooperative equilibria. *Automatica*, 23(4):523–533, 1987.